Northern Australia Environmental Resources Hub

National Environmental Science Programme

Ecohydrology and sensitivity of riparian flora, Magela Creek, Ranger uranium mine

Final report

Lindsay B. Hutley, Clément Duvert, Samantha A. Setterfield, Adam Bourke, Caroline A. Canham, Fiona L. Freestone, Ornela O. Cavalieri, Diego Alvarez-Cortez and Michael Brand

CHARLES DARWIN UNIVERSITY AUSTRALIA

THE UNIVERSITY OF WESTERN AUSTRALIA

Australian Government
Department of Agriculture, Water and the Environment

This report should be cited as:

Hutley LB, Duvert C, Setterfield SA, Bourke A, Canham CA, Freestone FL, Cavalieri OO, Alvarez-Cortez D and Brand M (2021) *Ecohydrology and sensitivity of riparian flora, Magela Creek, Ranger uranium mine*. Charles Darwin University, Darwin.

Cover photographs

Front cover: Ranger uranium mine lease area (photo: Patch Clapp).

Back cover: *Barringtonia acutangula* and *Pandanas aquaticus* plants in pot trial testing elevated levels of magnesium sulphate (photo Adam Bourke).

This report is available for download from the Northern Australia Environmental Resources (NAER) Hub website at nespnorthern.edu.au

The Hub is supported through funding from the Australian Government's National Environmental Science Program (NESP). The NESP NAER Hub is hosted by Charles Darwin University.

ISBN: 978-1-922684-06-6

September, 2021

Contents

List of tables

List of figures

Acronyms

ANSTO... Australian Nuclear Science and Technology Organisation

CDU..... Charles Darwin University

ERA..... Energy Resources of Australia Ltd

GDE..... Groundwater-dependent ecosystem

SSB..... Supervising Scientist Branch

UWA..... The University of Western Australia

Acknowledgements

We pay our respects to all Traditional Owners of Kakadu National Park where we conducted this study and acknowledge Elders past, present and emerging. We also wish to acknowledge the Gundjeihmi Aboriginal Corporation (GAC) for permissions to work on Mirarr Country, the Magela Creek catchment, Kakadu National Park. We also acknowledge the support of staff from the Australian Government's Supervising Scientist Branch (SSB) – Dr Andrew Harford, Dr Chris Humphrey, Dr Renée Bartolo, Ms Lisa Chandler and Ms Amie Leggett for their important input into the study, from design to interpretation of findings. SSB staff members Mr Lachlan Wyatt and Mr Alastair McCorkelle provided invaluable help during field campaigns at Magela Creek. Mr Peter Christophersen from Top End Native Plants Pty Ltd supervised the seed collection and germination and seedling propagation as well as provision of advice on species selection for the Magela Creek area. Members of the Djurrubu Rangers assisted during some of the field sampling. Thanks to Ms Michelle Iles and Mr David Staggs of Energy Resources of Australia Ltd (ERA) who provided us with various reports on the hydrology and geochemistry of the catchment.

Executive summary

Spring-fed monsoon vine forests and riparian (riverbank) vegetation are highly dependent on groundwater and provide essential habitat for highly diverse aquatic ecosystems. Contamination of shallow groundwater post-rehabilitation of the Ranger uranium mine site could therefore have significant impact on riparian vegetation and stream health of Magela Creek which runs through the mine lease and Kakadu National Park (Figure 1).

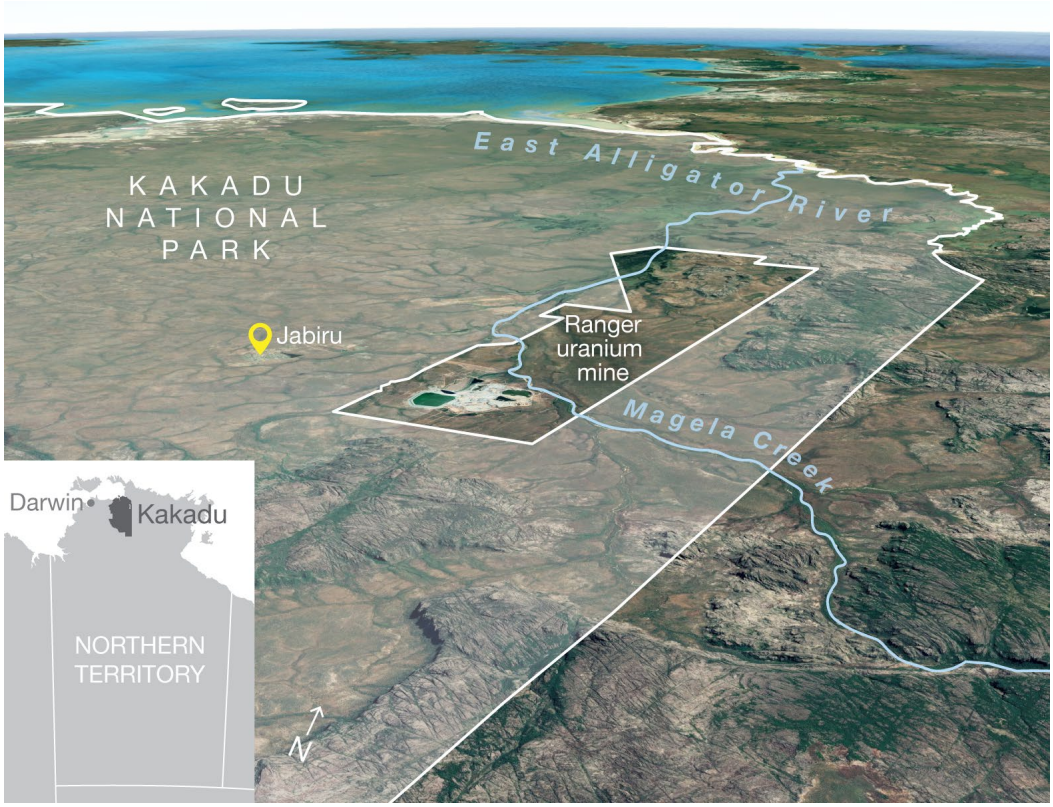

Figure 1. Location of Ranger uranium mine and Magela Creek adjacent to Kakadu National Park.

Environmental isotopes were used to quantify the groundwater dependence of riparian vegetation in the Magela Creek catchment. This knowledge was coupled with sensitivity testing of common riparian woody species to magnesium sulfate ($MgSO_4$ – a salt and the most likely contaminant in the mine wastewater) to provide a risk assessment of impact from potentially contaminated surface and/or groundwater.

Pit closure at Ranger is predicted to result in exfiltrating groundwater with elevated levels of $MgSO_4$ derived from waste rock. Solute modelling predicts that within 10 years of closure, groundwater reaching the surface waters of the freshwater Magela Creek may result in surface water with $MgSO_4$ concentrations >3 mg L^{-1}, in excess of the current desired exposure limits for surface waters (Sigda et al. 2013). This is a potential threat to the ecology of Magela Creek for any organisms that depend on surface water and/or groundwater. This project focused on risks posed to groundwater-dependent ecosystems, in particular the riparian vegetation of Magela Creek.

Project activity centred around two aims:

Aim 1. Use stable and radioactive isotopes to age and quantify water sources used by riparian vegetation within the Magela Creek catchment.

Aim 2. Undertake pot trials to examine the sensitivity of dominant riparian woody species to a wide range of $MgSO_4$ concentrations.

Stable isotopic mixing analyses suggest that riparian trees along Magela Creek predominantly access shallow (~0.7–1.5 m depth) soil water sources. However, the origin of this shallow soil water could be either wet-season rainfall or capillary rise from the groundwater below. Aside from this shallow soil water dominance, we found that trees located on ridges, islands and lower banks of the creek channel also use shallow groundwater contained in the sand-bed alluvial aquifer, while some of the trees located on the floodplain (about 40 m away from the channel) use groundwater contained in shallow parts of the weathered bedrock aquifer (Figure 2). Table 1 provides a summary of percentages of late dry-season water sources and shows considerable groundwater usage for several positions in the landscape.

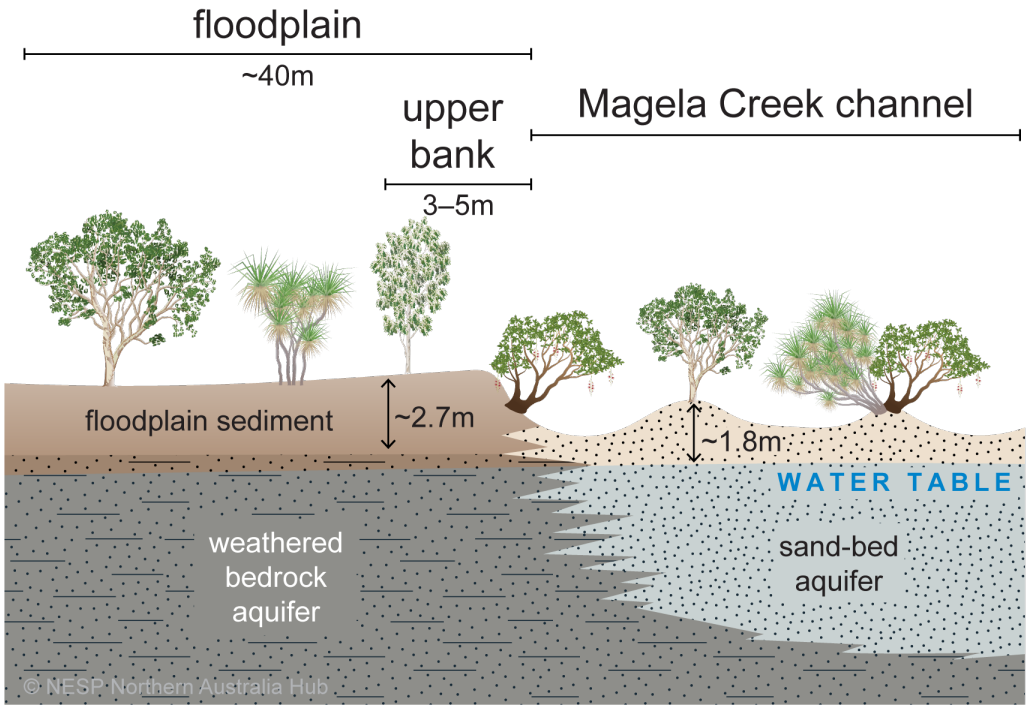

Figure 2.General morphology of Magela Creek in the dry season.

Table 1. Median percentages of late dry-season water sources utilised by riparian tree species partitioned across morphological positions of the Magela Creek channel. For each source, the approximate depth and range below ground is given. The shallow soil-water source for the channel position may be either wet-season rainfall infiltration or capillary action upwards from the groundwater below.

Location	Shallow soil water (0.7–1.5 m)	Deep soil water (1.5–3 m)	Sand-bed aquifer (1.5–2 m; in channel only)	Shallow bedrock aquifer (3–5 m)
Channel (ridges, islands, lower banks)	69–83%	—	14–26%	1–2%
Upper bank	89–95%	3–6%	—	1–3%
Floodplain	58–66%	20%	—	10–11%

Isotopic data also point to the potential of preferential flow pathways within and between geological layers and although there is no direct evidence for connectivity between the shallow weathered bedrock and alluvial sand-bed aquifers, hydraulic gradients suggest that subsurface flow from the shallow bedrock to the riparian area occurs during the wet season and flow recession. During the dry season, lateral connectivity is low as the creek ceases to flow and the vertical component of groundwater flow becomes dominant.

Given the potential for lateral inflow of contaminated groundwater from the shallow parts of the bedrock to the sand-bed aquifer during the wetter months, risk may be high for trees located in the channel (i.e. on ridges, islands and lower banks) due to their potential use of contaminated water present in the sand-bed aquifer and overlying soils. Risk may also be high in floodplain areas where trees are likely to use some bedrock groundwater under very dry conditions.

In summary, riparian trees predominantly use soil water during the dry season and varying amounts of groundwater. If these sources are contaminated (as they are presently at MC3, one of our study sites in Magela Creek that receives contaminated mine-derived groundwater), then mature trees will be exposed to that contamination. During the wet season, exposure may arise from contaminated groundwater and/or surface water from mine-site runoff or leachate. However, pot trial findings suggest that riparian species are unlikely to be severely impacted by $MgSO_4$ at (and even greater than) currently modelled concentrations, as no significant growth impacts were observed for $MgSO_4$ concentrations up to 7,095 mg L^{-1} $MgSO_4$ (equivalent to 1,433 mg L^{-1} Mg) across the eight species tested.

Scaling estimates from INTERA (2016) on potential solute egress suggest peak magnesium load from the rehabilitated landform could reach 500 mg L^{-1} Mg in shallow groundwaters. This value has a high uncertainty, and an updated value is required to provide a more realistic threshold to provide context for the pot trial findings. This concentration sits between two of our experimental treatments (T4 [394 mg L^{-1} Mg] and T5 [789 mg L^{-1} Mg]) and findings from whole-plant growth and leaf-scale physiology indicate tolerance at these concentrations across all species screened. Canham et al. (2020) reported a 30% decline in biomass for *Alphitonia excelsa* (red ash) between 1 and 194 mg L^{-1} Mg – declines which were also reflected in gas exchange measures. As this was the only species that showed impact in these trials, testing was repeated with five treatment concentrations up to 789 mg L^{-1} Mg. This additional trial showed little evidence of impact, similar to the behaviour of the other seven species, suggesting risks from $MgSO_4$ contamination to common riparian species could be reasonably classified as low.

1. Introduction

Groundwater-dependent ecosystems (GDEs) have been defined by Richardson et al. (2011:92) as 'natural ecosystems that require access to groundwater to meet all or some of their water requirements on a permanent or intermittent basis, so as to maintain their communities of plants and animals, ecosystem processes and ecosystem services'. Given the highly seasonal nature of rainfall in northern Australia, it is not unreasonable to assume most vegetation has some degree of groundwater dependence, in particular riparian vegetation associated with rivers and ephemeral streams that must survive the dry season.

Previous work has focused on understanding the potential of groundwater dependence of dominant northern Australian vegetation systems, including tropical savanna open forests and woodlands, riparian vegetation and monsoon vine forests (Cook et al. 1998; Eamus et al 2000; Hutley et al 2000; Kelley 2002; Kelley et al 2007; Liddle et al. 2008; O'Grady et al 2006).

O'Grady et al. (2006) examined groundwater dependence of riparian and monsoon vine forests that occupy bank environments of the Daly River, Northern Territory (NT). On this major river, riparian vegetation exhibited distinct zonation as riverbanks are steep (20–40 m in height) with a series of terraces from the river, and there was considerable structural and floristic complexity as a function of position in landscape. Sap-flow measurements revealed a high degree of spatial variability and ranged from 1.8 to over 4.0 mm d^{-1}. The isotopic signature of deuterium ($\delta^{18}O$) of xylem water was compared with soil pore water, river water and groundwater and a mixing model suggested groundwater dependence was estimated at 59–75% in the dry season (O'Grady et al. 2006). The magnitude depended on position, with high levels of groundwater use by trees closer to the river relative to trees higher on the levees.

Liddle et al. (2008) took a similar approach to examine the groundwater usage of spring-fed monsoon vine forest in the Darwin region. Water use by monsoon vine forest trees and partitioning of this flux into soil and groundwater sources were investigated by examining $\delta^{18}O$ values of groundwater, soil water and tree xylem water samples. A two-component mixing model was used to partition sources. As with O'Grady et al. (2006), dry-season stand transpiration was estimated from individual tree sap-flow measurements scaled by basal area and ranged from 1.8 to 2.0 mm d^{-1}, with 45% sourced from groundwater. Variations in water use and proportion of groundwater sourced between sites were attributed to the floristic and structural attributes of each patch of monsoon vine forest as opposed to historical groundwater extraction.

Such studies suggest there is a high probability that riparian vegetation of the Magela Creek catchment may be similarly dependent on groundwater. This proposition is also supported by the Groundwater Dependent Ecosystems Atlas (Richardson et al. 2011, bom.gov.au/water/groundwater/gde/map.shtml) which suggests riparian areas will have a high GDE potential, with billabong and seasonal wetlands a moderate-to-low potential (Doody et al. 2017). Savanna woodland areas were deemed to have limited to no groundwater dependence, consistent with root excavations in savanna and soil water balance studies (Eamus et al. 2002; Kelley 2002) which suggested savanna vegetation is largely supported by rain-fed deep (3–5 m) soil moisture sources.

Toxicity of $MgSO_4$ has also been the subject of previous studies, with limits for aquatic vegetation (algae and macrophytes) examined (Begg et al. 2001; McCullough 2006; van Dam et al. 2010). However, there is little to no knowledge of levels that woody riparian species can tolerate (Canham et al. 2020), a significant knowledge gap given the potential for groundwater contamination post-rehabilitation and the significant reliance on groundwater during the late dry season. In this study, we combined an assessment of riparian tree groundwater dependence and susceptibility of sapling growth to high levels $MgSO_4$ concentrations via pot trials to assess risk posed by the predicted exfiltration of groundwater with elevated levels of $MgSO_4$ sourced from the rehabilitated mine landform.

2. Methodology

2.1 Aim 1: Water sourcing and aging – stable and radioactive isotope analysis

Water sourcing

The stable isotopes of water ($\delta^{18}O$ and $\delta^{2}H$) have been widely used to estimate the relative contributions of different water sources to xylem water of vegetation. Contributions of soil pore water, river/creek water, surface or deep groundwater can be determined by matching their isotopic signature with that of water taken up by vegetation of interest (e.g. O'Grady et al. 2006). Recently, probabilistic models based on Bayesian hierarchical modelling techniques have been developed to assess the likelihood of source proportions that incorporate source variability (Phillips and Gregg 2003; Parnell et al. 2013; Stock et al. 2018). This class of mixing models has been increasingly used for vegetation source water identification (e.g. Barbeta et al. 2015; Evaristo et al. 2016). In this more sophisticated approach, mixing model formulations provide probabilistic solutions to the mixing system and are not limited by the simple ratio of sources to tracers (i.e. under-determined systems). Observed variability in both source and mixture tracer signatures is integrated in the model (Stock et al. 2018). Here we used MixSIAR, a linear mixing model embedded in a Bayesian framework, to determine the relative contributions of each water source to xylem water of different tree species present within the riparian corridor. The model was run for three landscape positions (see details in the following section) to determine the influence of landscape position on tree water sources and to account for differences in soil isotopic compositions between positions.

We considered three potential sources (soil pore water at different depths and either sand-bed or shallow bedrock aquifer depending on the landscape position). Prior to using the isotopic composition of each potential source (both $\delta^{18}O$ and $\delta^{2}H$) as model inputs, some of the isotopic data had to be corrected. Firstly, we corrected for the isotopic offset between bulk and unbound soil water using the empirical formulations developed by Chen et al. (2016). This correction is required because plant water sourcing studies based on bulk soil water isotopic measurements may lead to inaccurate estimates of source proportions since some of the more tightly bound soil water may not be available for trees.

Secondly, we corrected for the observed depletion in $\delta^{2}H$ in all xylem water samples. There is growing empirical evidence that xylem water can be depleted in $\delta^{2}H$ relative to source water (e.g. Evaristo and McDonnell 2017; Geris et al. 2017; Barbeta et al. 2019), and these authors recommend numerically correcting this depletion prior to application of mixing models (Barbeta et al. 2019; Li et al. 2021; Hahn et al. 2021). To do this, we computed a composite 'source water line' similar to Li et al. (2021) based on all potential sources. Instead of calculating different offsets for each sample as in Li et al. (2021), we used an average offset for all samples in order to keep some of the natural variability across samples.

Groundwater residence times

Tritium (^{3}H) is a radioactive isotope of hydrogen that can provide reliable estimates of water age up to ~100 years and detect groundwater contributions to streamflow (Duvert et al.

2016). Groundwater aging can help assess recharge processes and dominant flowpaths to Magela Creek – and ultimately these data can assist with modelling surface and groundwater interactions in the mine area. A selection of bores intersecting the bedrock aquifer at different depths (maintained by mine operator Energy Resources of Australia Ltd [ERA]) and piezometers positioned in alluvial sands of Magela Creek (~2 m depth and operated by the Australian Government's Supervising Scientist Branch [SSB]) were sampled for ^{3}H analysis (Table 2; Figure 3).

We used measurements of ^{3}H in rainfall taken monthly at Darwin airport by the Australian Nuclear Science and Technology Organisation (ANSTO) between 1963 and 2017 as the initial input of ^{3}H in the groundwater system. We assumed that ^{3}H activity in Darwin is equivalent to that in the study area. These historical rainfall measurements were used to assess the current ^{3}H activity of past rainfall events by accounting for the natural radioactive decay of ^{3}H (decay rate 0.0567 y^{-1}). We also decided to use the ^{3}H activities measured in groundwater as a proxy for groundwater residence times. Estimating groundwater residence times would require the use of a lumped parameter model, which would come with a-priori assumptions and introduce additional uncertainties (Suckow 2014). The modelling approach would also provide non-unique results that may vary between tracers. Therefore, the direct interpretation of ^{3}H activity, rather than an indirect estimate of residence time, was considered more appropriate here (Suckow 2014).

Field sampling

Two riparian sites along Magela Creek were chosen in consultation with SSB staff, both within the Ranger Project Area (MC1 and MC3; Figure 3A). The MC1 site is located upstream of Pit 3 while MC3 is further downstream near the junction with Coonjimba Billabong. Most sampling was undertaken at MC3 because of the three clearly defined terraces at this site. Soil and twig samples were taken across the three terraces or landscape positions: on a ridge located within the channel, next to a network of SSB piezometers and about 1 m above the lowest parts of the channel (referred to as 'channel' in the following; water table ~1.8 m below ground), in the upper part of the riverbank, that is, 3–5 m away from the channel and over 2 m above the lowest parts of the channel ('upper bank'; water table ~2.7 m below ground), and within the floodplain about 40 m away from the channel ('floodplain'; water table ~2.8 m below ground; Figure 3B). In the channel, soil and twig samples were taken within a small radius (1–3 m) of the piezometers that were used to collect sand-bed groundwater samples. Most sampling was conducted at the end of the dry season in September 2019.

At each position, three replicate holes were dug using a hand auger, each hole being 3–5 m apart. From each hole, soil samples were collected at approximately 0.3–0.4 m intervals and until the capillary fringe was reached. Holes were consistent in depth within replicates, and the deepest sample was collected at 3.1 m (floodplain). All soil samples were double-bagged and refrigerated on site. Samples were collected in duplicate, with one used for soil matric potential, gravimetric water content and particle size distribution measurements and the other for isotopic analyses.

Table 2. ERA bores and SSB piezometers with screen depths sampled for ^{3}H analysis. Bore locations are marked on the sampling map, Figure 3.

Bore ID	Screen depth (m)
MCP07	<2
MC12	0.3-3
MC11	0.3-3.5
MS3B	0.5-3.5
P3-3C	10-16
P1C-OB1C	11-14
MC27D	12-18
MC12D	18-24
P3-3B	21-27
P3-10B	21-33
P3-15B	22-30
P1C-OB1B	26-29
P3-5	29-41
OB96-A	36-38
P3-16	37-52
P3-3A	40-52
OB95-B	41-45
P3-15A	42-54
P3-12	56-71
P1C-OB1D	103-106

We sampled five of the most common riparian tree species in the study area (Table 3, Figure 4). Because we opted for species that are common across the whole riparian environment, we did not sample some of the species that grow immediately adjacent to the low points in the channel and that are likely to be most reliant on groundwater, such as *Pandanus aquaticus* and *Syzygium* spp. At the floodplain landscape position, only two species (*Melaleuca viridiflora* [broad-leaved paperbark] and *Lophostemon lactifluus* [swamp mahogany]) were present, while *M. alternifolia* (narrow-leaved paperbark) was present only at the channel landscape position. At each site and landscape position we sampled three replicate trees per species and two replicate twigs per tree. We collected twigs of approximately 10–15 mm diameter from the canopy using a telescopic pruner. These were cut into 200–250 mm lengths and immediately wrapped in parafilm, sealed with electrical tape, double-bagged and refrigerated on-site.

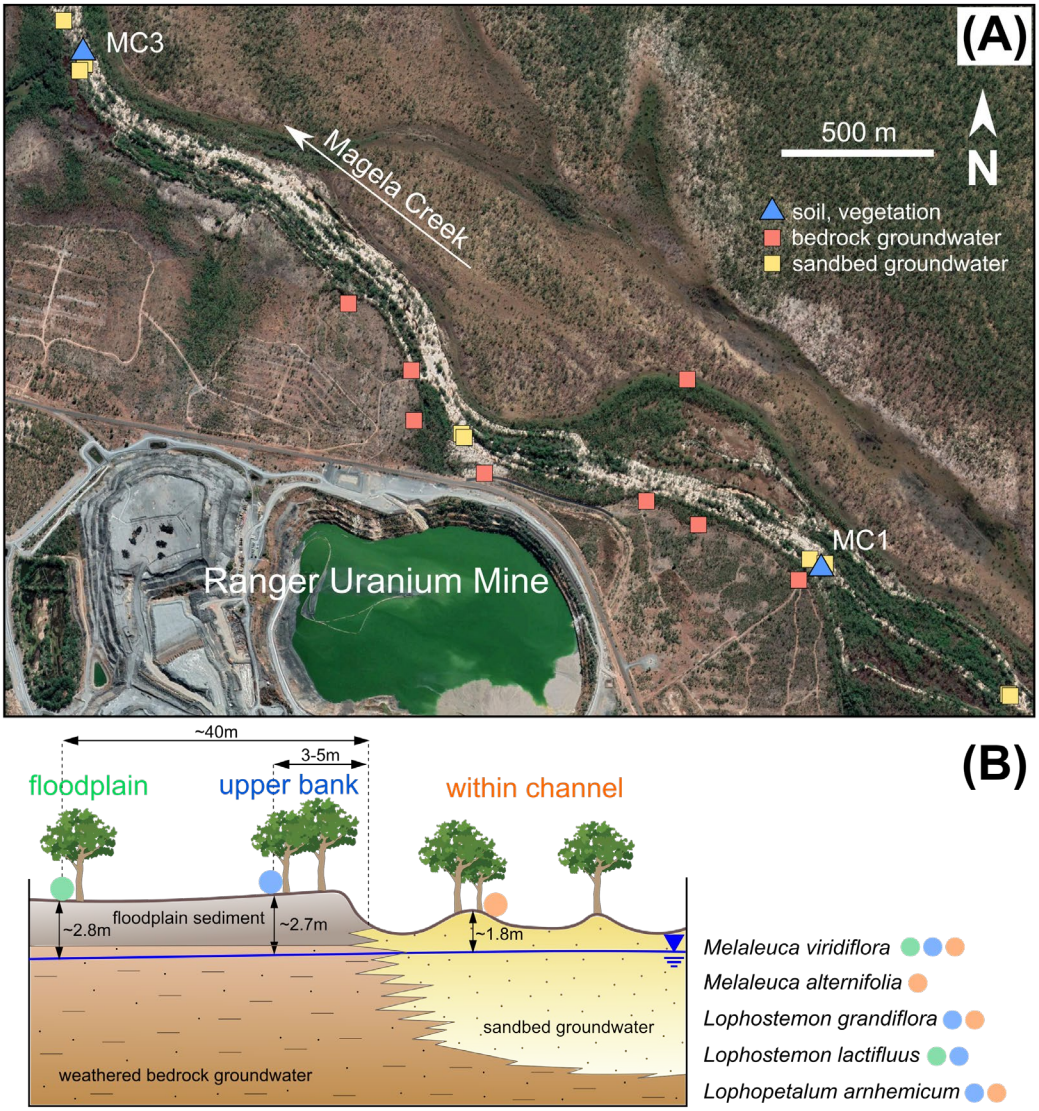

Figure 3. (A) Locations of the two sampling sites along Magela Creek (MC1, MC3) where soil and twig samples were taken (blue triangles) and locations of groundwater bores and piezometers along the creek (red and yellow squares). (B) Conceptual cross-section of MC3 showing the three locations where groundwater, soil and tree twigs were collected. The blue line represents the water table depth.

A total of 19 ERA bores and one SSB piezometer were sampled for stable isotopes and ^{3}H analyses (Table 2), with five additional SSB piezometers sampled for stable isotopes. The selected bores are screened at different depths, from about 5 m to over 60 m below the ground. A submersible pump (Tornado, Proactive) was used to take samples once three bore volumes had been purged or once pH and conductivity had stabilised. In order to develop a local meteoric water line, rainfall sampling was undertaken weekly during the 2019–2020 and 2020–2021 wet seasons by SSB staff at their Jabiru Field Station. A total of 28 rainfall samples were obtained and subsequently analysed for stable isotopes at Charles Darwin University.

Table 3. Riparian tree species sampled for each landscape position at MC3.

Species	Within channel	Upper bank	Floodplain
Melaleuca viridiflora	X	X	X
Melaleuca alternifolia	X		
Lophostemon grandiflora	X	X	
Lophostemon lactifluus		X	X
Lophopetalum arnhemicum	X	X	

Soil measurements

Gravimetric soil water content and matric potential (Ψ_m) were measured to further constrain the mixing model, as soil that is below a moisture threshold is unlikely to provide source moisture to trees regardless of its isotopic value. For all soil samples collected, samples were dried at 105°C for 96 hours. The Ψ_m was estimated using the filter paper method as described in Deka et al. (1995). A filter paper (Whatman No. 42) was placed in an airtight sealed container surrounded by the soil sample and was left at constant temperature for 14 days to ensure a matric potential equilibrium between the filter paper and soil sample was reached. Gravimetric water contents were used with the calibration curve in Deka et al. (1995) to obtain Ψ_m in MPa. Samples with a Ψ_m below -3 MPa were excluded from the isotopic database and were not included in the mixing model as it was assumed that at this tension, uptake of moisture by woody vegetation was not possible.

To correct for the isotopic fractionation between adsorbed and unbound water in the soil (Chen et al. 2016; Barbeta et al. 2020), the fraction of sand in our soil samples was determined. This was done using a Hielscher ultrasound ring-sonotrode. Dried samples were transferred into the sieve tower and two sieve sizes were used (4.75 and 0.075 mm) so that only the sand fraction was retained and quantified.

Isotopic analyses

Water samples were analysed for $\delta^{18}O$ and $\delta^{2}H$ at Charles Darwin University using a cavity ring-down spectrometer fitted with a diffusion sampler (Picarro Inc., Santa Clara, CA, model L2130-I; Munksgaard et al. 2011). The isotopic differences between various materials (e.g. xylem water, groundwater) are very small, so isotopic composition is reported relative to an internationally accepted standard (Vienna Standard Mean Ocean Water, VSMOW) and expressed in parts per thousand δ (‰). Deviation from that standard ratio is given as:

$$\delta\ (‰) = (R_{sample} / R_{standard}) - 1)) \times 1000;$$

where R is the ratio of heavy-to-light isotope, with R_{sample} and $R_{standard}$ the isotopic ratios in the sample material and standard. The $\delta^{18}O$ and $\delta^{2}H$ raw values were normalised to the VSMOW scale based on three laboratory standards and reported in per-mil (‰). The analytical uncertainty was determined as <1.0‰ for $\delta^{2}H$ and <0.1‰ for $\delta^{18}O$.

Water was extracted from soil and twig samples at the West Australian Biogeochemistry Centre (University of Western Australia) using cryogenic vacuum distillation following the procedure in West et al. (2006). Samples were heated (>90°C) under vacuum and water vapour was caught in a liquid nitrogen cold trap. Extraction times were 60 and 90 min for soil and twig samples, respectively. In parallel, water was extracted from four different standards

following the same procedure for quality control. Extracted samples were then analysed using the Picarro L2130-I (Piccaro Inc.) in the same laboratory.

All ^{3}H samples were analysed at ANSTO in Sydney. Samples were distilled and electrolytically enriched around 70-fold prior to counting with a liquid scintillation counter for several weeks. The limit of quantification was 0.07 tritium units (TU) for all samples, and analytical precision was between ±0.03 and ±0.06 TU.

2.2 Aim 2: Sensitivity of riparian vegetation to $MgSO_4$ – pot trials

Design and trial establishment

Pot trials were undertaken using a standard randomised block design to test the sensitivity of seven common riparian tree species (Figure 5) to a wide range of $MgSO_4$ concentrations that spanned three orders of magnitude (5–7,096 mg L^{-1} $MgSO_4$). Media, pot design and watering regimes were tested in an initial trial design at The University of Western Australia (UWA) glasshouses using two targeted species, *M. viridiflora* and *A. excelsa* as described by Canham et al. (2020). Plants were grown in cylindrical pots using a washed-sand media with nutrient delivery and $MgSO_4$ concentration manipulation achieved via the use of a modified Hoagland solution (Smith et al. 1983). Using a nutrient solution in a washed-sand culture provided the ideal mechanism to control and balance nutrient levels, provide non-limiting moisture and manipulate $MgSO_4$ concentration in the growing media.

Pot trials were conducted over three phases. Trial species, treatment numbers and trial duration are given in Table 4. The phase I trial was carried out at UWA using two species, followed by phase II where a further four species were tested at the shade house facility at Charles Darwin University (CDU) Casuarina campus (Figure 4). The final phase III trial included two additional species *Pandanus aquaticus* (river pandanus) and *Barringtonia acutangula* (freshwater mangrove) plus a re-testing of *A. excelsa* (Table 4) using a narrower range of treatment concentrations than the phase I trial. Species were selected in consultation with SSB staff and Kakadu Native Plants Pty Ltd, with seed sourced from the Magela Creek catchment in Kakadu National Park in collaboration with Kakadu Native Plants Pty Ltd. Canham et al. (2020) described the planting design for the phase I trial and a similar methodology was adopted for the phase II and III trials.

Collected seeds were subsequently germinated by Kakadu Native Plants staff with seedlings transported to CDU's Casuarina shade house. The seedlings were transplanted to the 1 m experimental pots when they were ~10–15 cm in height. Once transplanted, a further 2-week establishment period was undertaken using a standard low nutrient solution (modified Hoaglands solution, see Appendix 1) to ensure root establishment prior to exposure to the treatments. Pots were 100 x 20 cm with washed sand used as a potting media (Figure 4, Figure 6).

Figure 4. Phase II pot trial at CDU shade house. Four species were grown in a randomised block design of seven $MgSO_4$ treatments with six replicates per treatment per species.

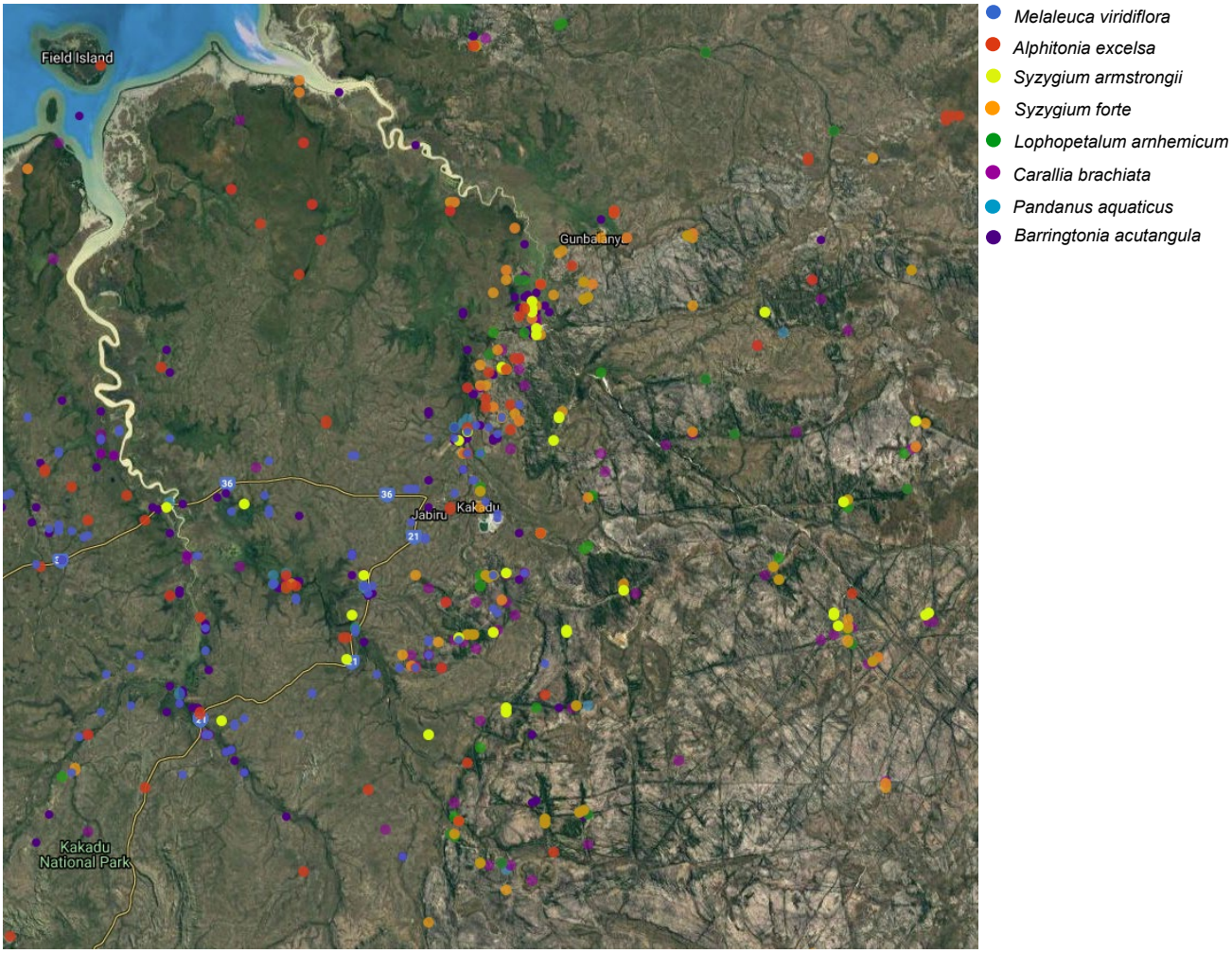

Figure 5. Distribution of selected riparian species for the pot trials and their distribution in the Magela Creek catchment area. Plant occurrence data was sourced from the Atlas of Living Australia database (https://spatial.ala.org.au?ss=1628227908051). Species occurrence is strongly associated with drainage channels and low-lying areas, except for A. excelsa*, which occurs in both riparian and non-riparian areas.*

Each species was exposed to seven $MgSO_4$ treatments (T1–T7; 5.1, 69.2, 467.0, 961.8, 1,954.2, 3,907.2 and 7,096 mg L^{-1} $MgSO_4$ respectively), with six replicate pots established per treatment concentration per species. On advice from SSB staff, the Mg:Ca ratio in the Hoagland solution was set at 9:1 after van Dam et al. (2010). In the phase I trial at UWA, calcium levels were not adjusted and the Mg:Ca ratio increased with treatment (Canham et al. 2020). A single plant was cultivated per pot. Treatment solutions were applied to pots via 450 mL applications twice per week. This was a small variation from the phase I trial which had small pot volumes and treatment solutions were applied daily to pots in an enclosed glasshouse. The solution volume used in phase II and III trials was set to result in a small drainage from the pot base suggesting the media was at or near field capacity following watering. Plant wilting was not observed between waterings. At high treatment concentrations, T6 and T7, magnesium precipitate was observed on the soil surface and at the bottom of the pot due to evaporation of drained nutrient solutions (Figure 6). This was evident during the dry-season months, and pots were flushed every 3–4 weeks with water to 'reset' nutrient and $MgSO_4$ concentrations within the media to prevent accumulation of salts over and above designed concentrations.

In the phase III trial, sand media was slightly finer than phase II, with softer-leaf species tested (Table 4) requiring three solution applications per week. The phase I trial outcomes were reported in Canham et al. (2020), with a limited response from *M. viridiflora* to $MgSO_4$ concentration, whereas *A. excelsa* showed a significant impact at concentrations from 960 mg L^{-1} $MgSO_4$. Given this outcome, we included *A. excelsa* in the phase III trial, but we used T1 to T6 treatments, excluding T7. This enabled testing over a lower but more detailed range of magnesium concentrations than was used in the phase I trial.

Measurements

Plant height to apical tip was measured every three weeks for the duration of phase II and III trials. Plants were harvested at eight months as there was evidence of inhibited growth and root binding within the pot. Plants were harvested for total above-ground biomass. Prior to harvest, three young and three old leaves were sampled from three replicate individuals per species for foliar elemental analysis after Canham et al. (2020). At harvest, mean plant height and biomass data we reused to test for a response to $MgSO_4$ concentration. A Shapiro-Wilk test for normality was undertaken followed by a one-way analysis of variance (ANOVA) with Tukey honestly significant difference (HSD) post hoc tests. Where necessary, data were square-root transformed.

Table 4. Riparian tree species used in each phase of the pot trials undertaken at UWA and CDU. Note A. excelsa *was included in two trials.*

Phase	Species	Location	$MgSO_4$ treatments	Trial duration (months)
I	*Melaleuca viridiflora*	UWA	7	2.5
	Alphitonia excelsa		4	
II	*Syzygium armstrongii*	CDU	7	8
	Syzygium forte		7	
	Lophopetalum arnhemicum		7	
	Carallia brachiata		7	
III	*Pandanus aquaticus*	CDU	7	9
	Barringtonia acutangula		7	
	Alphitonia excelsa		6	

Figure 6. Magnesium precipitate on pots in high concentration treatments. Arrows show precipitate on a) the soil surface of a S. armstrongii *pot at T6, 3,907 mg* L^{-1} $MgSO_4$*, b) on the soil surface of* C. brachiata *pot at T7, 7,096 mg* L^{-1} $MgSO_4$*, and c) at the base of a T7 treatment pot. Pot flushing with water was undertaken when precipitate was observed during the dry-season months of the trials.*

Plant stress was assessed using leaf fluorometry. The degree of leaf fluorescence indicates stress-induced imbalances between light absorption and the use of energy in photosynthesis. Stress in this experiment was potentially due to ionic imbalances and metabolic impacts arising from exposure to the range of $MgSO_4$ concentrations. A gas analyser (Li-Cor Li6400 XT, LI-COR Biosciences, Lincoln, USA) equipped with a leaf chamber fluorometer (Li6400-40, LI-COR Biosciences) was used to examine leaf fluorescence. For all species, six replicate leaves from the control treatment plants (T1, 5 mg L^{-1} $MgSO_4$) and the highest treatment (T7, 7,096 mg L^{-1} $MgSO_4$), were assessed using the commonly measured Fv/Fm, the ratio of variable fluorescence (Fv) to maximum fluorescence (Fm) induced by a high light pulse on dark adapted leaves (Schreiber et al. 1986). Mature leaves were dark adapted overnight and measures of Fv/Fm were undertaken from 9.30 am to noon local time the following morning.

3. Results

3.1 Isotopic analysis of tree water sources

Stable isotope signatures

The isotopic compositions of rainfall, xylem water and source water are shown in dual-isotope space (Figure 7). An evaporation trend was apparent for soil samples and xylem water, with waters gradually departing from the meteoric water line. Samples taken from the saturated zone in the sand-bed channel also followed the evaporation trend. This pattern reflects the shallow nature of water contained in these components and their direct contact with the atmosphere. The wide range of values observed in the sand-bed aquifer may be a result of spatial heterogeneities in sunlight exposure and depth to groundwater, with less shaded areas and/or near-surface water tables more prone to evaporative enrichment. In contrast, groundwater in the bedrock was more isotopically depleted and plotted closer to the meteoric water line. Depleted isotopic signatures in groundwater have been associated with recharge following heavy rainfall events (Harrington et al. 2002; Sánchez-Murillo and Birkel 2016), suggesting that the bedrock aquifer was predominantly recharged by large, isotopically depleted monsoonal events with negligible evaporation. One likely recharge pathway for the bedrock is when surface water in Magela Creek flows over the banks and onto the floodplain (i.e. overbank flow recharge; Doble et al. 2012). Localised upwellings of depleted bedrock groundwater into the sand-bed aquifer may be another factor contributing to the spatial variability in the sand-bed groundwater isotopic values.

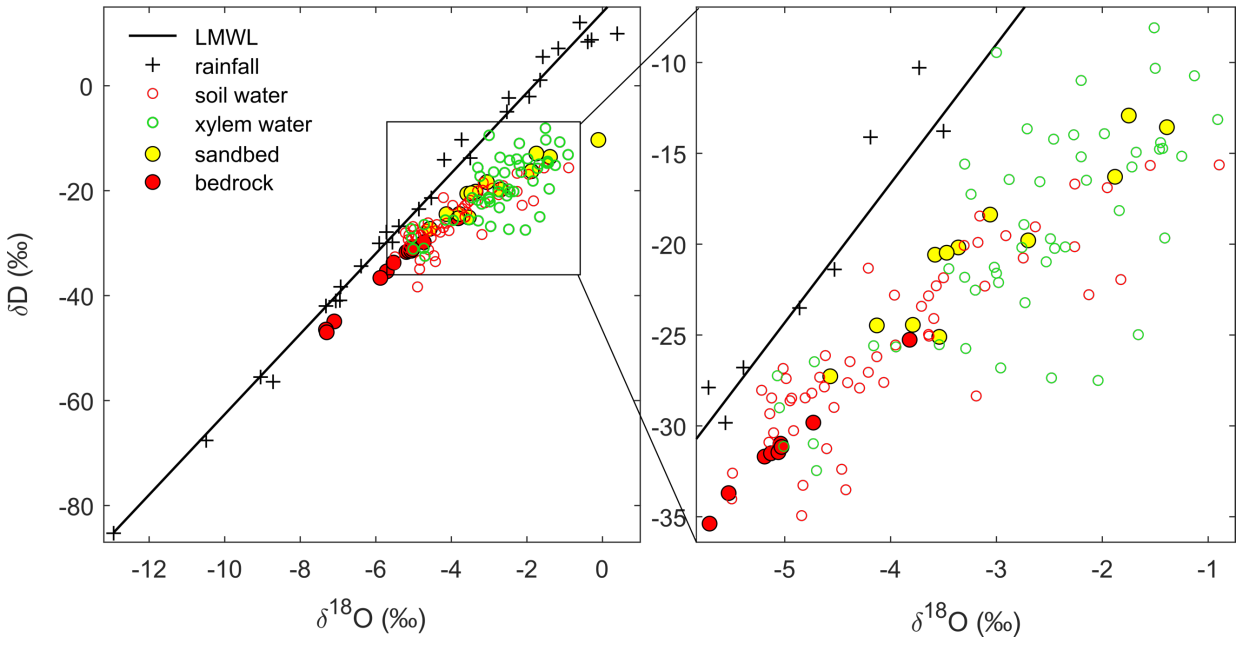

Figure 7. Isotopic composition of rainfall, xylem water, soil water, sand-bed groundwater and bedrock groundwater at Ranger uranium mine. Both the soil and xylem water isotopic ratios reported in this figure correspond to corrected values (see methods). Only soil samples for which Ψ_m >-3 MPa are shown. The local meteoric water line (LMWL) is $\delta^2H = 7.66\ \delta^{18}O + 13.99$, obtained as a linear regression function based on 28 rainfall samples collected between 2019 and 2021.

The isotopic composition of soil water was strongly controlled by its position in the landscape (Figure 8). While soil taken from the creek channel had enriched (evaporated) isotopic signatures ($\delta^{18}O$ between -4 and 0‰), soil taken further away from the channel at the top of the riverbank and in the floodplain area had more depleted signatures, plotting closer to bedrock groundwater ($\delta^{18}O$ between -6 and -2‰). For all positions in the landscape there was also a general trend of stronger isotopic enrichment at shallower soil depths (Figure 8). The isotopic composition of xylem water seemed to align well with the isotopic composition of shallow soil water and that of sand-bed groundwater in the channel, for both $\delta^{2}H$ and $\delta^{18}O$.

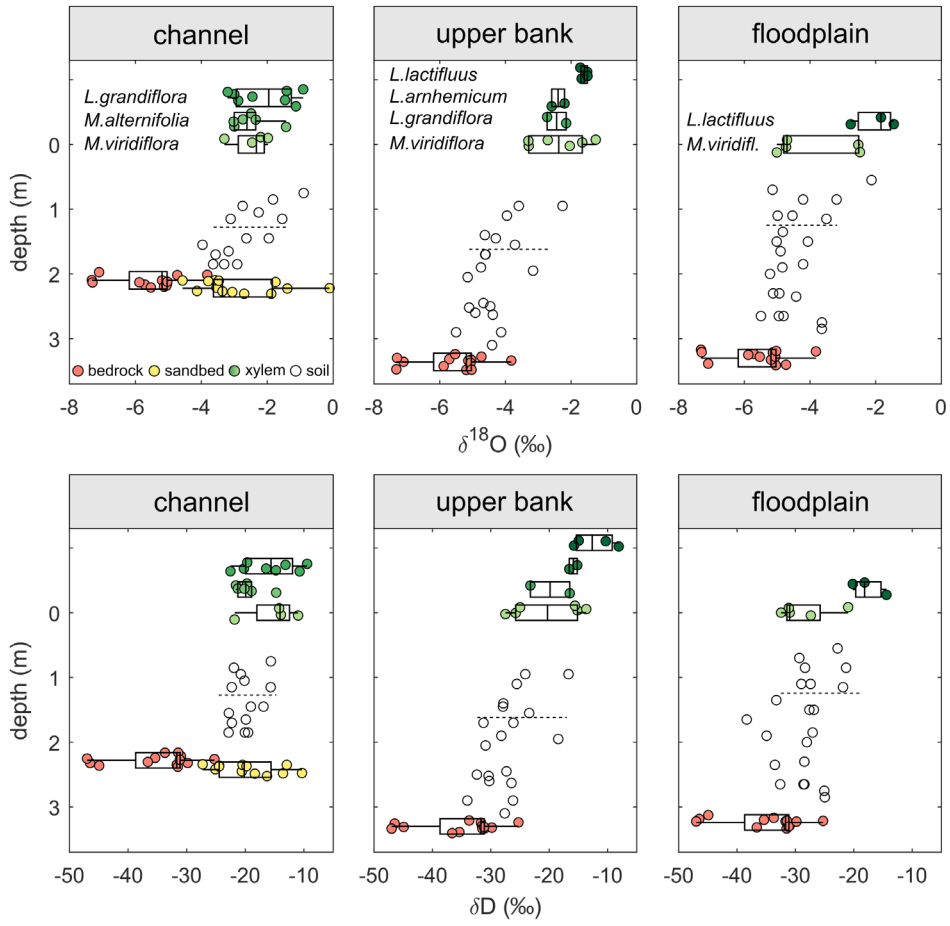

Figure 8. Soil water isotopic ratios (white circles) measured along four (upper bank) and three (channel and floodplain) replicate soil profiles. Data are shown for $\delta^{18}O$ (top) and $\delta^{2}H$ (bottom) and for each landscape position. Boxplots show the distribution of isotopic values in xylem water for each tree species (shades of green), sand-bed groundwater (yellow) and bedrock groundwater (red). Boxes correspond to the median and interquartile range and whiskers represent the minimum and maximum values. Dashed lines represent the separation between shallow and deep soil for the mixing analyses. The y-axis (depth) is relevant only for soil data.

Mixing analyses

Soil water isotopic compositions did not differ significantly between MC1 and MC3 for the upper bank, but there were significant differences in $\delta^{18}O$ values between the two sites for the channel landscape position (Table 5). Therefore, for the upper bank position we combined soil isotopic ratios from MC1 and MC3 as the inputs for soil water sources in the mixing models (with a total of one MC1 core and three MC3 cores), whereas for the channel

position we only used the three MC3 cores. Likewise, we found no statistical difference between the isotopic composition of xylem water collected at MC1 and MC3 (Table 5), so we pooled all xylem water data together for the mixing model analyses in an effort to obtain more robust and reliable outputs.

For all landscape positions, we separated soil water data into shallow and deep soil since differences were significant for at least one of the two isotopes (Table 5). The separation between shallow and deep soil was set at 1.2 m, 1.5 m and 1.1 m for the channel, upper-bank and floodplain, respectively. This separation is indicated on Figure 8 as a dashed line for each location and isotope. In the channel, we grouped deep soil and saturated soil (i.e. sand-bed groundwater), because differences between these two groups were not significant (Table 5). This likely reflects capillary action in the deep soil horizons, which led us to consider this source as a groundwater source after Doody et al. (2017). While shallow soil water was considered as a distinct source in the channel (Table 5), we cannot completely rule out the possibility that this shallow soil water was capillary water too. We removed the sand-bed groundwater as a potential source at the upper bank and floodplain positions, because, due to the distance and ready availability of other, closer sources (i.e. shallow and deep soil moisture), this source was unlikely to be accessed by trees.

Table 5. Results of the two-sample t-tests to assess isotopic differences between groups. At each position in the landscape, we grouped data from three replicate soil profiles for each depth (shallow and deep), while for the sand-bed groundwater source in the channel we considered a subset of data taken from four piezometers located in the vicinity of MC3 (i.e. where corresponding soil samples were collected). All p-values in bold and italic are significant at the 95% confidence level, meaning that the two groups considered are significantly different.

Sample type	Location	p-value ($\delta^{18}O$)	p-value ($\delta^{2}H$)
Soil	Channel (MC1 *vs* MC3)	***0.00003***	0.23
	Upper bank (MC1 *vs* MC3)	0.56	0.53
	MC3 channel (shallow soil *vs* deep soil)	***0.017***	0.47
	MC3 channel (deep soil *vs* sand-bed)	0.58	0.64
	MC3 channel (shallow soil *vs* sand-bed)	***0.00002***	***0.000001***
	MC1+MC3 upper bank (shallow soil *vs* deep soil)	***0.015***	***0.049***
	MC3 floodplain (shallow soil *vs* deep soil)	***0.007***	***0.018***
Twigs	Channel (MC1 *vs* MC3)	0.92	0.21
	Upper bank (MC1 *vs* MC3)	0.35	0.47
	Floodplain (MC1 *vs* MC3)	0.47	0.95

We found that the differences in source water contributions between tree species were not as significant as the differences between positions in the landscape (Figure 9). For trees

located on the ridges, islands and lower banks of the creek channel, xylem water was sourced from a mixture of shallow (0.7–1.2 m) soil water (range of median relative contributions across species and based on 3,000 Monte Carlo simulations 69–83%; see the entire distributions for each species in Figure 7) and sand-bed groundwater (range of median relative contributions across species 14–26%). Again, the shallow soil-water source may also originate from capillary action, although a capillary fringe of >1 m in height (as would be needed here to explain the presence of shallow soil moisture) is relatively unlikely in coarse sand (Malik et al. 1984; Liu et al. 2014; Hird and Bolton 2017). Under the assumption that shallow soil water does originate from capillary rise, then the contribution of groundwater to tree water uptake in the channel would be >98% for all species. For trees located on the upper bank away from the channel, shallow soil water located at 0.9–1.5 m was the dominant (range of median relative contributions across species 89–95%) source, with deeper soil water contributing a minor (range of median relative contributions across species 3–6%) fraction to tree uptake. Due to the high availability of soil moisture at shallow depths, bedrock groundwater was a negligible source of water for trees located in the channel and on the upper bank. In the floodplain area, trees were found to use a mixture of shallow (range of median relative contributions across species 57–66%) and deeper (median relative contributions 20% for both species) soil water, with potentially a minor (range of median relative contributions across species 10–11%) contribution from bedrock groundwater (Figure 9).

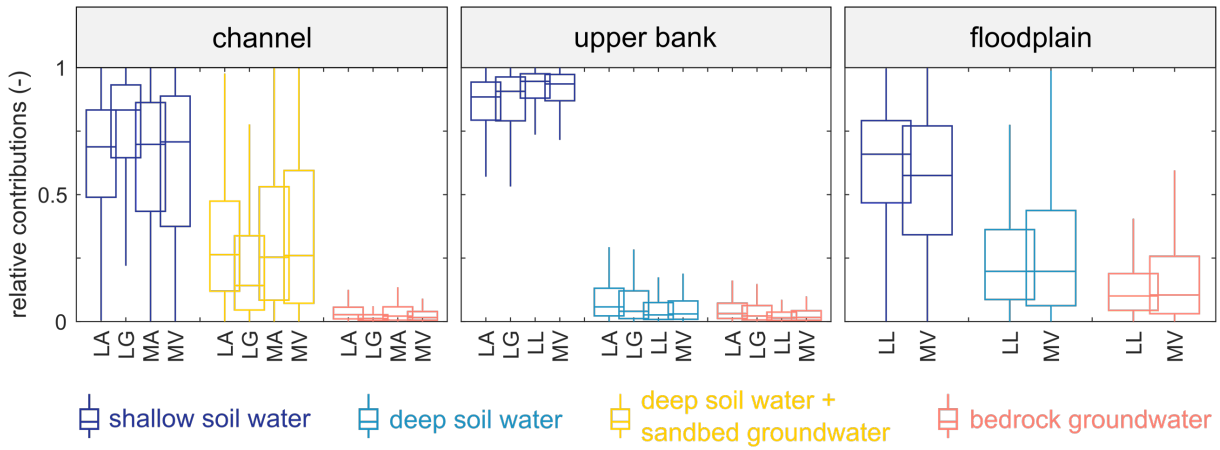

Figure 9. Results of mixing model analyses used to determine the relative contribution of each water source at MC3 per tree species and landscape position. 'LA' is for Lophopetalum arnhemicum*, 'LG' for* Lophostemon grandiflora*, 'LL' for* Lophostemon lactifluus*, 'MA' for* Melaleuca alternifolia *and 'MV' for* M. viridiflora*. Only soil samples for which Ψ_m >-3 MPa were considered in the soil water sources. The boxplots correspond to minima, maxima, medians and interquartile ranges based on 3,000 Monte Carlo simulations in MixSIAR.*

Groundwater flow paths and residence times

High ^{3}H activities were measured in rainfall in the 1960s as a result of nuclear testing (Figure 10). Since then, ^{3}H activity in the atmosphere has considerably declined and has now returned to background levels, with current values stabilising around 1 TU in Darwin. Most of the sampled bores had ^{3}H activities below or similar to that of recent rainfall. The bores intersecting very shallow layers of either the alluvium (MCP07) or the bedrock (MC11 and MC12) had activities slightly above the activities in current rainfall. These can be considered as representative of current rainfall on-site (i.e. recent recharge), as we expect that rainfall in

RUM would be slightly more enriched in ^{3}H than rainfall in Darwin (Tadros et al. 2014). About a third of the bores we sampled had ^{3}H activities between 0.4 and 0.8 TU, suggesting relatively recent waters that were recharged in the last 10–30 years. Eight other bores had much lower ^{3}H activities (<0.27 TU) indicative of longer residence times in the subsurface and waters most probably recharged before the 1960s.

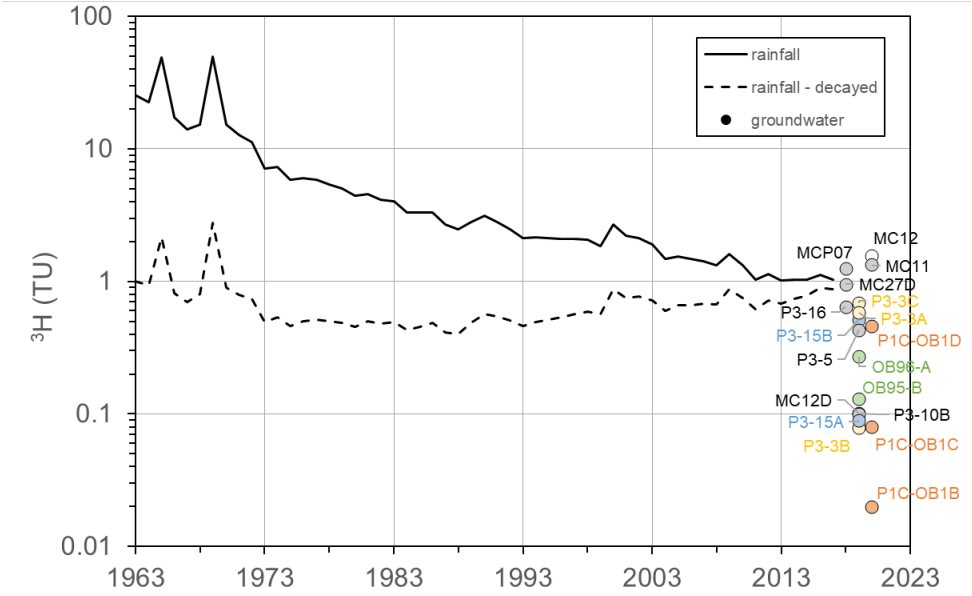

Figure 10. Tritium (^{3}H) activity measured in rainfall (Darwin airport) since 1963 (black line) and current (2020) ^{3}H activity of these past inputs (dashed line). The markers correspond to ^{3}H activity measured in bores across the study area. Markers with the same colour represent nested bores.

We found a negative correlation between ^{3}H and the bore screen depth (Figure 11). Bores located at depths <10 m had the highest ^{3}H activities, while some of those intersecting the bedrock aquifer between 40 and 50 m had values below 0.2 TU. This means that waters at depth are consistently older than waters near the surface, suggesting that the dominant flow component is vertical (Cartwright et al. 2006). However, some bores did not follow this general pattern. A cluster of outliers (highlighted in orange in Figure 11) includes five bores with depths around 20–30 m and unexpectedly low ^{3}H compared to other bores at similar depths. We hypothesise these long residence times at relatively shallow depth are due to the presence of less permeable geological materials at these depths, hence lower hydraulic conductivities. According to Ahmad and Green (1986), clayey horizons in some areas of the bedrock give a semi-confined characteristic to the groundwater.

A second cluster of outliers (highlighted in green in Figure 11) includes two bores with higher ^{3}H activities than other bores at similar or shallower depths. Preferential flow pathways in layers with high hydraulic conductivity and/or through cracks or fractures may locally connect the surface and deeper bedrock layers. The similar ^{3}H activity in P3-3A and P3-3C (nested bores) is an illustration of the possible connection between different layers within the bedrock. The relatively high 3H activity measured in the deepest bore we sampled, P1C-OB1D, may also be explained by leaks along the bore casing or by the presence of faults/fractures connecting shallow and deep layers of the bedrock in this area.

Overall, the highly variable ^{3}H activities we found in the deep bedrock aquifer reflects the considerable spatial heterogeneity in this geological formation, with varying lithologies and hydraulic conductivities, in line with findings from Ahmad and Green (1986) and Leaney and Puhalovich (2006). Further data are needed to better constrain flowpaths within and between aquifers, and the interface between the sand-bed sediment in the channel and bedrock aquifers would require particular attention.

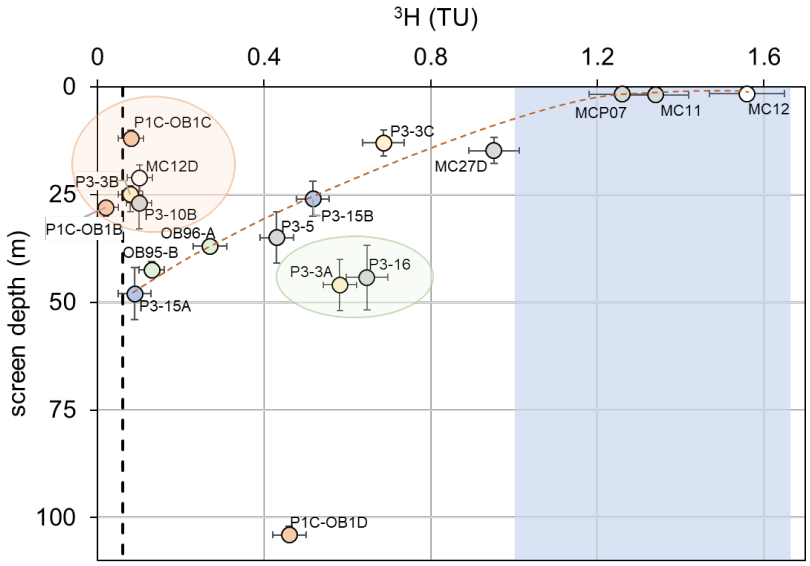

Figure 11. Relationship between ^{3}H and bore screen depth. Markers with the same colour represent nested bores. The orange dashed line represents the general trend of decreasing ^{3}H activity (i.e. increasing residence time) with increasing depth. The vertical bars around each marker represent the screen depth ranges for each bore, and the horizontal bars relate to the ^{3}H measurement uncertainty. The black dashed line represents the lower limit of quantification (0.06 TU) while the blue area to the right represents the likely range of current ^{3}H input (rainfall).

3.2 Testing riparian species sensitivity to $MgSO_4$ exposure – pot trials

Plant growth performance

Mean plant height over time and above-ground biomass at harvest for the seven species tested in the phase II and III trials are shown in Figure 12 to Figure 18. Plant performance, be it change in height or more importantly biomass, showed negligible impact from elevated $MgSO_4$ relative to the control treatment (T1). All species showed a positive growth response up to treatment T3 or T4, although this increase was only statically significant for *P. aquaticus* (ANOVA, $F_{8,33} = 9.53$, $P < 0.01$) at T6 (27.5% greater biomass than T1, $P<0.01$) and T7 (18.7% greater biomass T1, $P=0.059$, Figure 13). Declines in biomass were evident in T7 (7,095 mg L^{-1}) for *S. armstrongii* and *Lophopetalum arnhemicum* of ~20% and 15% respectively, but these differences were not significant.

The plant height to biomass ratio (H:D) was examined for all treatments and species to examine changes to allocation patterns (Figure 19). Most species showed no significant change, the exception being a significant decrease (pseudo-F =3.2, P = 0.02) in the H:D of *A. excelsa* with $MgSO_4$ concentration (Figure 19). Statistical tables are given in Appendix 1.

At harvest, the root mass of individual plants from phase II and phase III trials were washed and photographed to examine any morphological differences. Images are provided in Appendix 2. No morphological differences were observed except for some darker colouring of the T6 plants of *A. excelsa* (Appendix 2, Figure 4).

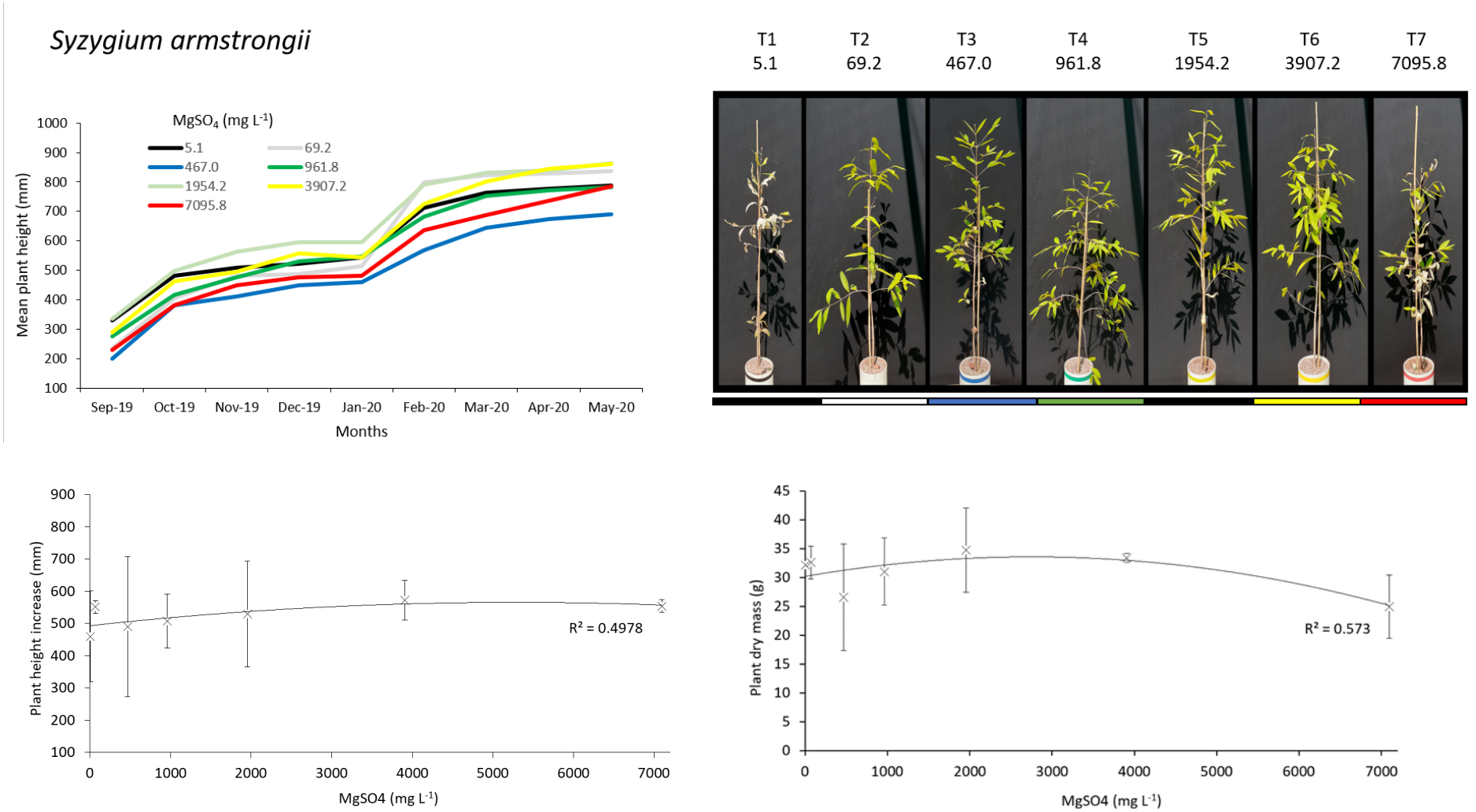

Figure 12. *Plant height through time and with $MgSO_4$ treatment concentrations and biomass data at harvest for* Syzygium armstrongii. *Photographs are of a typical individual for treatments T1 to T7 at final harvest, with treatment concentrations given in mg L^{-1} $MgSO_4$.*

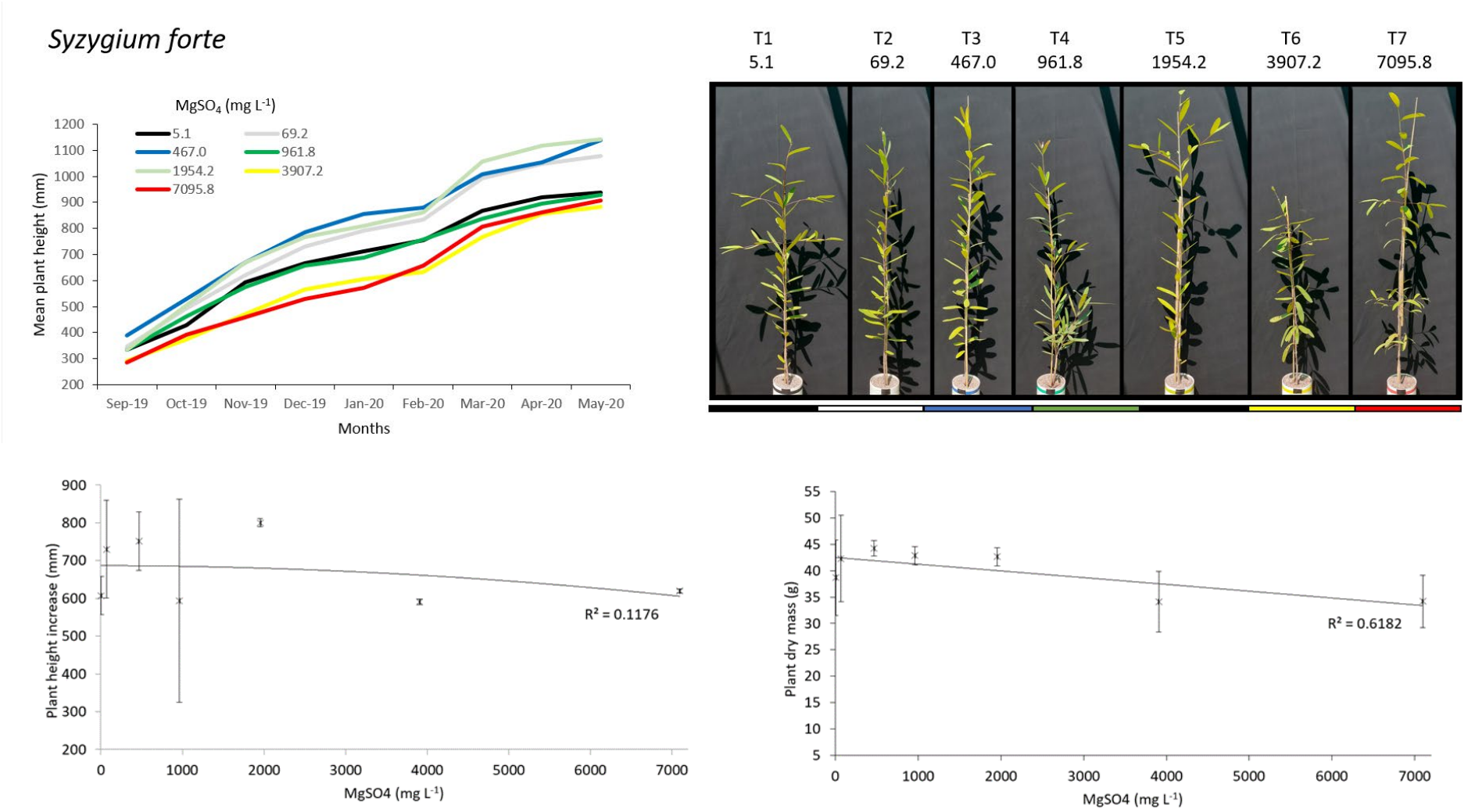

Figure 13. *Plant height through time and with $MgSO_4$ treatment concentrations and biomass data at harvest for* Syzygium forte *Photographs are of a typical individual from each treatment at final harvest. Treatment concentrations are as given in Figure 12.*

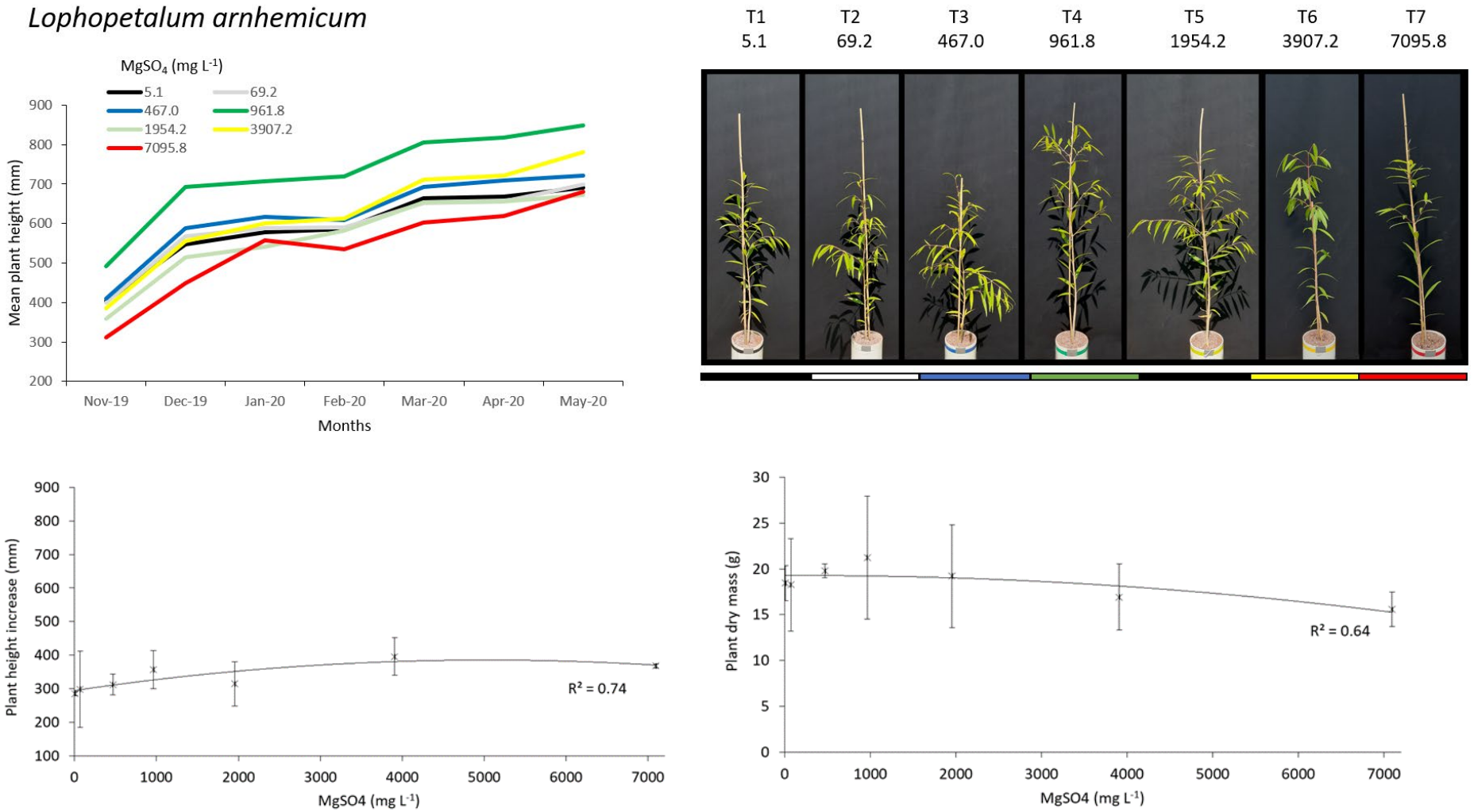

Figure 14. *Plant height through time and with $MgSO_4$ treatment concentrations and biomass data at harvest for* Lophopetalum arnhemicum. *Photographs are of a typical individual for each treatment at final harvest. Treatment concentrations are as given in Figure 12.*

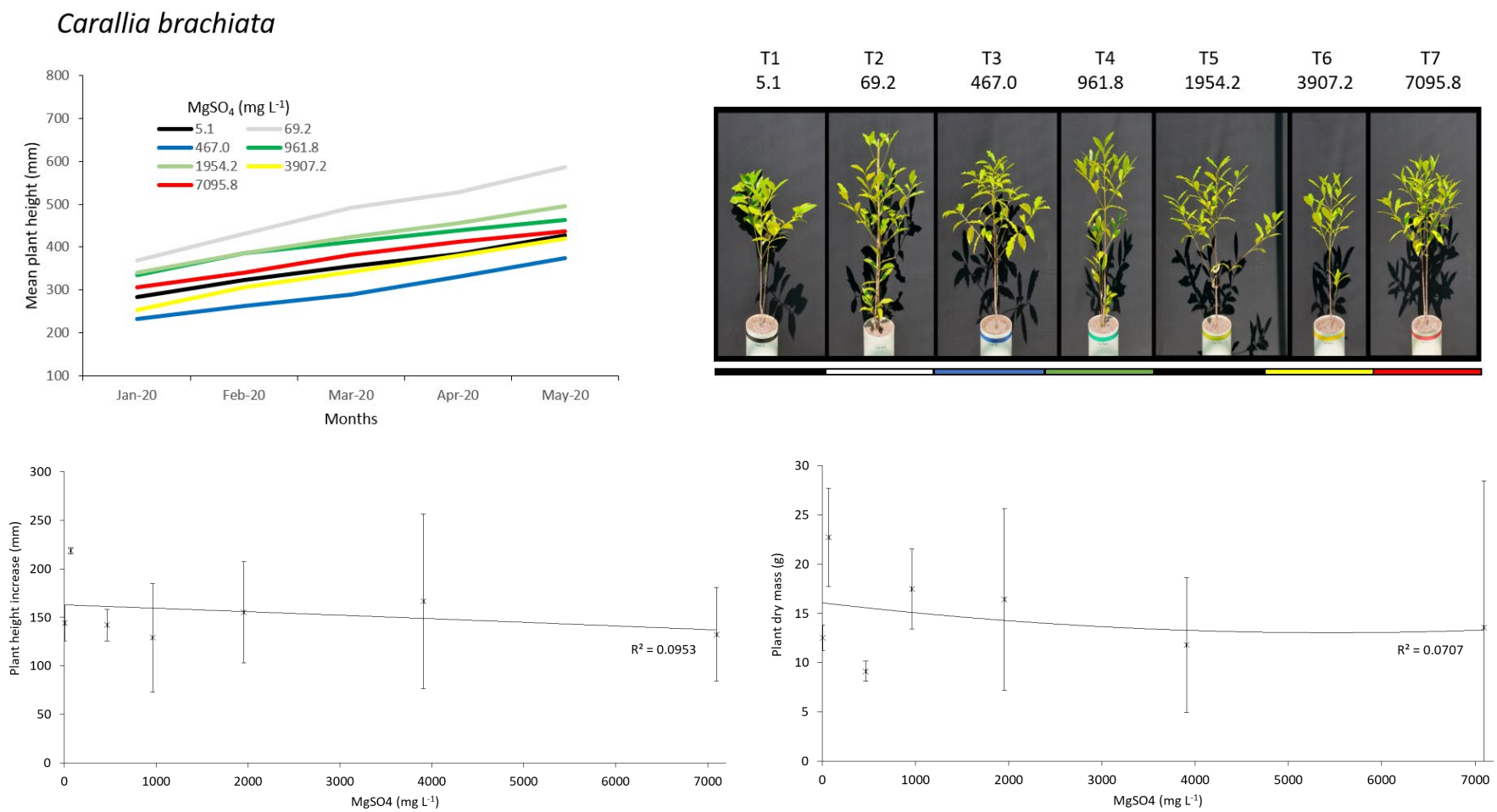

Figure 15. *Plant height through time and with $MgSO_4$ treatment concentrations and biomass data at harvest for* Carallia brachiata. *Photographs are of a typical individual for each treatment at final harvest. Treatment concentrations are as given in Figure 12.*

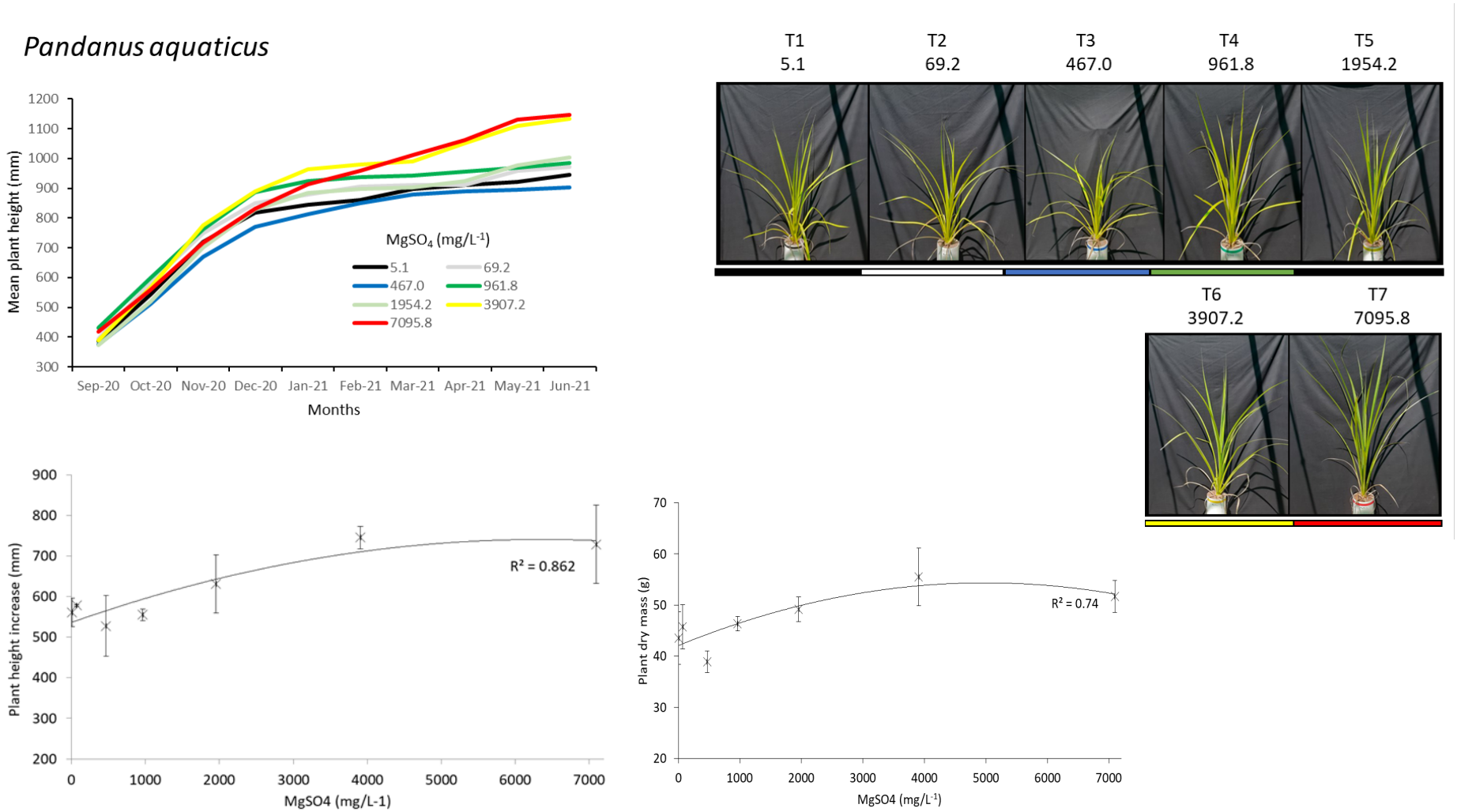

Figure 16. *Plant height through time and with $MgSO_4$ treatment concentrations and biomass data at harvest for* Pandanus aquaticus. *Photographs are of a typical individual for each treatment at final harvest. Treatment concentrations are as given in Figure 12.*

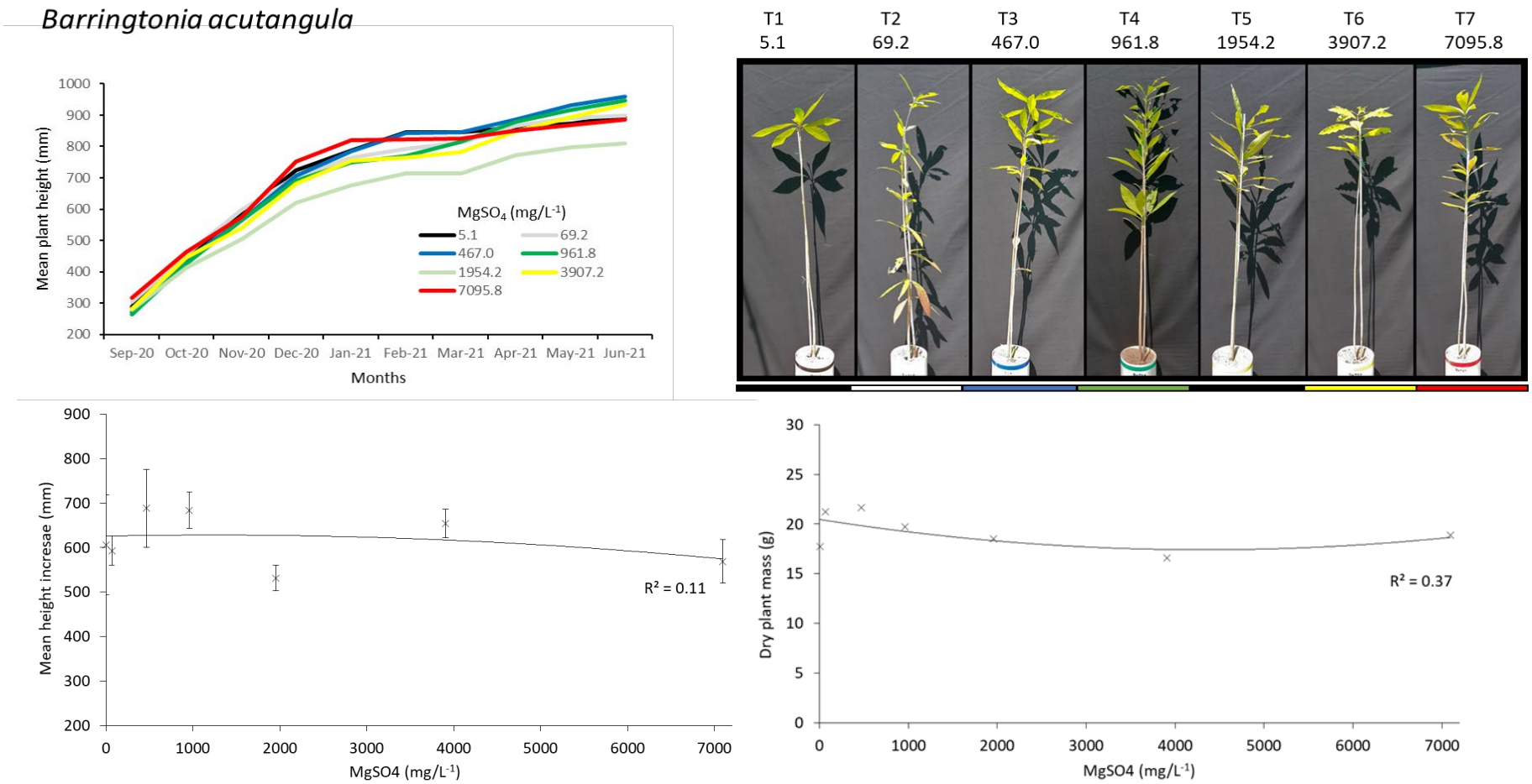

Figure 17. *Plant height through time and with $MgSO_4$ treatment concentrations and biomass data at harvest for* Barringtonia acutangula. *Photographs are of a typical individual for each treatment at final harvest. Treatment concentrations are as given in Figure 12.*

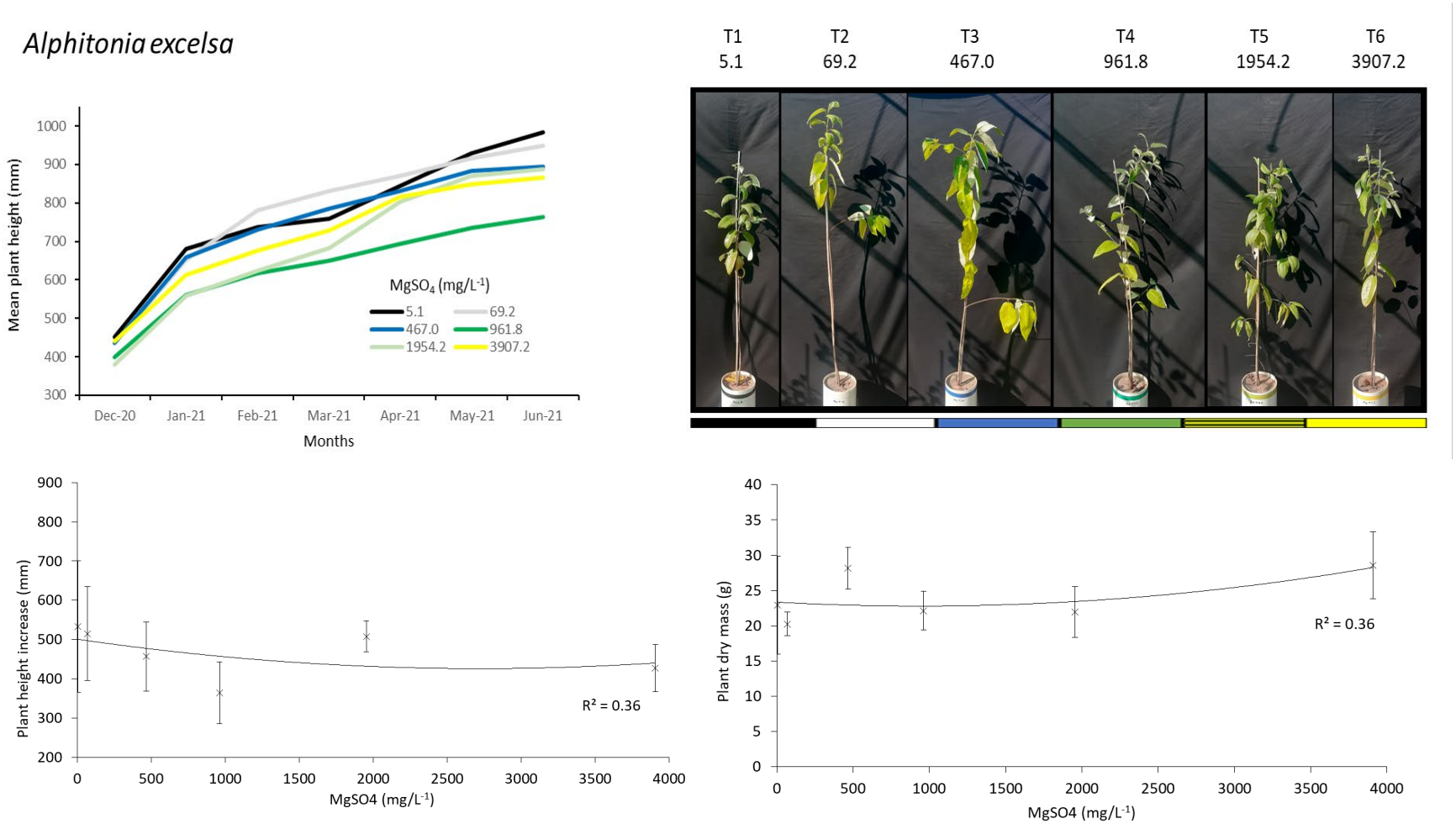

Figure 18. *Plant height through time and with $MgSO_4$ treatment concentrations and biomass data at harvest for* Alphitonia excelsa. *Photographs are of a typical individual for each treatment at final harvest. Treatment concentrations are as given in Figure 12.*

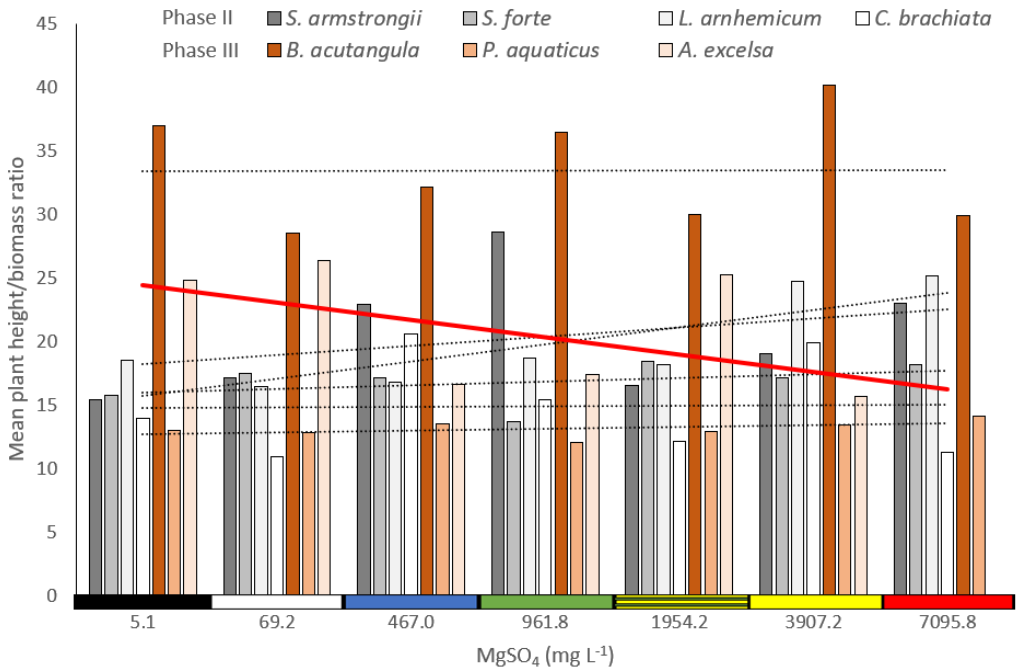

Figure 19. *Ratio of mean plant height to biomass (H/B) for all species at the final harvest.* Alphitonia excelsa *was the only species to show a decline in H/B, with regression line for this species shown in red.*

Leaf fluorescence

Further assessment of plant performance was undertaken using leaf fluorescence measures via quantification of the Fv/Fm ratio. Values of this ratio range from 0.74–0.83 in non-stressed C3 leaves (Schreiber et al. 1986). Mean Fv/Fm for the four species of the phase II and III trials is given in Figure 20.

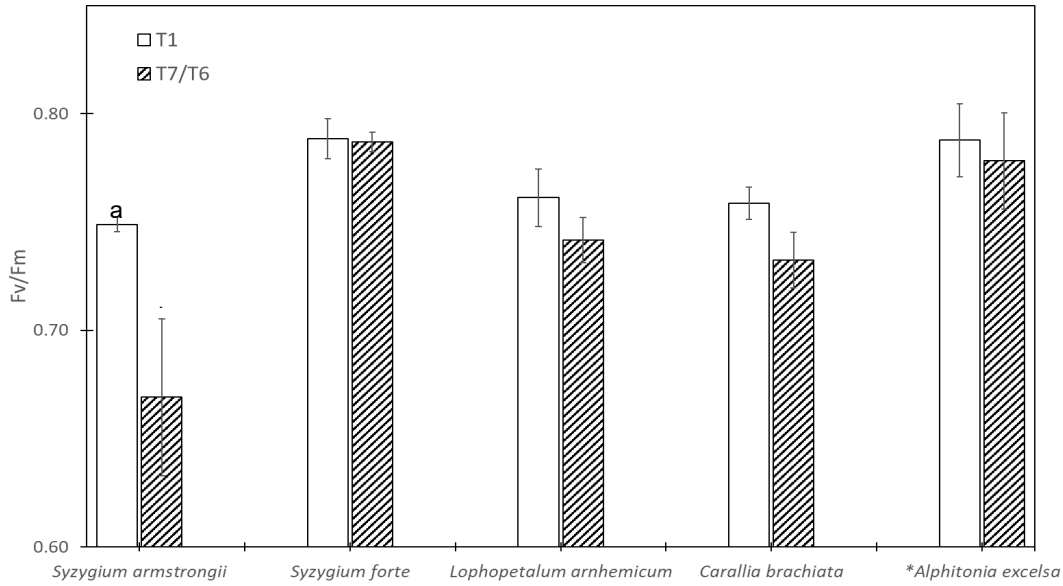

Figure 20. *Mean leaf fluorescence ratio Fv/Fm dark adapted leaves for T1 (control) and T7/T6 leaves for each species. Differing means are indicated for P<0.05 using a one-way ANOVA for T1 vs T7 ratios.* *A. excelsa *values are for T6, the highest concentration tested (3906 mg L^{-1}).*

The observed range of Fv/Fm was 0.73–0.81 across all treatments and species except for *S. armstrongii* at T7, which had mean value of 0.67, significantly different to T1 leaves. This suggests some degree of stress in *S. armstrongii* and is consistent with a reduced biomass in this species at the highest $MgSO_4$ concentration relative to the control (although this biomass difference was not significant). Fluorescence measures for all other species fell within a non-stressed range (~0.80).

4. Discussion

4.1 Groundwater dependence of riparian woody species

Our results show that the riparian trees we sampled along Magela Creek predominantly used soil moisture sourced from 0.7 to 1.5 m depth. In the channel, soil moisture may have a groundwater origin due to capillary action from the shallow water table into the upper layers of the soil profile. However, uncertainties remain regarding the origin of this soil moisture, as studies have reported maximum capillary rise heights of 20–80 cm in sand (Malik et al. 1984; Hird and Bolton 2017), whereas in our case, soil moisture was available for trees > 1 m above the water table. In any case, soil water was supplemented with varying contributions of groundwater, depending on the position in the landscape. We found that trees located on ridges and islands within the creek channel accessed significant amounts of shallow groundwater contained in the sand-bed alluvium. We also found some instances of shallow bedrock groundwater use in the floodplain area, although this source was minor.

For trees located on the upper bank of Magela Creek, we found no apparent groundwater use. This can be related to the sandy loam soil type at this location which resulted in high plant-available soil moisture from about 0.9 m depth. It is important to note, however, that the sand-bed groundwater was somewhat 'out of reach' of the trees we sampled in this upper section of the bank. We expect that riverbank trees located closer to the creek channel (i.e. on the lower part of the riverbank) would also be accessing sand-bed groundwater, as suggested by observations of riverbank trees with surface roots that reach the creek edge. We also expect that some of the species growing in the channel that we did not sample, such as *Pandanus aquaticus* and *Syzygium spp*., are reliant on shallow sand-bed groundwater too.

The reliance of riparian trees on groundwater at the end of the dry season has been reported in studies conducted in the wet–dry tropics of northern Australia (Lamontagne et al. 2005; Cook and O'Grady 2006; Canham et al. 2021), and our results add to this body of literature. Our finding that soil water remained a major source of tree water uptake at the end of the dry season on the upper bank and floodplain and for the species we examined was somewhat unexpected but is in line with our soil moisture and matric potential data. On the upper bank and in the floodplain, we estimate that the plant available water store was at least 100 mm at the end of the dry season. Given the likely transpiration rate for *M. viridiflora* is less than 1.5 mm d^{-1} in the late dry season (Kelley et al. 2007), exclusive reliance on soil water is a realistic assumption for these trees. It is possible, however, that under drier conditions following several consecutive low rainfall years, the soil moisture pools may become depleted and groundwater may become a more important source of water for trees located at these landscape positions.

Our ^{3}H results point to the potential of preferential pathways within and between geological layers, a result of the considerable heterogeneity of the subsurface. Although we found no direct evidence for connectivity between the bedrock and alluvial sand-bed, subsurface flow from the shallow bedrock to the riparian area may occur during the wet season and flow recession. Tritium and stable isotope data in these two components were indeed similar, and hydraulic gradients suggest lateral flow towards the creek in those periods. Subsurface connections are also known to occur downstream of the Coonjimba Billabong, with sand-bed groundwater clearly affected by contaminated subsurface inflows from the mine (Chandler et al. 2021). Given the potential for inflows of shallow bedrock groundwater into the sand-bed

formation, the risk of exposure to contaminants may be high for riparian trees, as our modelling shows that they are likely to rely on shallow groundwater during the dry season. The risk may be particularly high for trees located near the left bank of the creek channel, that is, the bank closest to subsurface inflows from the mine.

4.2 Impact of $MgSO_4$ on plant growth

Magnesium is an essential plant nutrient and is typically deficient in natural and agricultural ecosystems, and previous work is dominated by studies addressing deficiencies rather than an abundance or even toxicity (Canham et al. 2020). Pot trial findings suggest that riparian species are unlikely to be severely impacted by $MgSO_4$ as declines in biomass at high treatments were modest. Most species showed an enhanced growth response up to treatment T4 (395 mg L^{-1} Mg, equivalent to 1,954 mg L^{-1} $MgSO_4$), consistent with the physiological benefits of adequate to high magnesium supply, including increased photosynthesis, a role in loading and transport of photoassimilates into sink organs such as roots, shoot tips and seeds (Hermans et al. 2004), enzyme activation, and the formation and utilisation of ATP and positive effects on N-uptake (Cakmak and Kirkby 2008). Above T4, declines in biomass relative to the control (T1) were small and not significant.

The magnesium concentration at T4 is similar to estimates of the maximum potential solute egress from the rehabilitated landform, which could reach 500 mg L^{-1} in shallow groundwater. This threshold is based on magnesium concentrations in shallow groundwaters beneath the trial landform given in (INTERA 2016) scaled to the area of the rehabilitated landform (900 ha). This threshold has a high uncertainty, and further modelling is required to validate this value. This concentration sits between our T4 (394 mg L^{-1} Mg) and T5 (789 mg L^{-1} Mg) treatments and findings from whole-plant growth and leaf-scale physiology indicate tolerance at these concentrations across all species screened.

Canham et al. (2020) reported a 30% decline in biomass for *A. excelsa* between 1 and 194 mg L^{-1} Mg, declines which were also reflected in gas exchange parameters. As this was the only species from the phase I trial to show an impact, testing was repeated in the phase III trial with six treatment concentrations up to 789 mg L^{-1} Mg. In contrast to the result of Canham et al. (2020), impacts on growth in the phase III trial showed no significant difference across treatments. Reasons for this difference are unclear. *A. excelsa* did exhibit a significant ($P<0.02$) decline in the height-to-biomass ratio with increasing $MgSO_4$, which was due to a decrease in plant height rather than biomass. A reduction in height may indicate a preferential allocation to the root mass, perhaps indicative of an ionic imbalance and stress at high magnesium loads. However, there were no apparent differences in root morphology (Appendix 2, Figure 4), nor above-ground productivity.

Results on growth performance found here suggest little impact of magnesium concentrations up to 1,400 times higher than the control treatment that was set at or near current background levels of Mg <5 mg L^{-1}. This is also 2.6 times our estimated potential solute egress magnesium load from the rehabilitated landform. Based on currently available modelled concentrations, this suggests impacts on common woody riparian species from high levels of $MgSO_4$ in groundwater or surface water would likely be low.

5. Recommendations and conclusions

Stable isotopic mixing analyses suggest riparian trees along Magela Creek use a combination of soil water and shallow groundwater from either the sand-bed alluvium (channel) or the bedrock formation (floodplain). Table 1 provides a summary of percentages of late dry-season water sources and shows median uptakes of groundwater ranging from 1% to 26% dependent on position in the landscape. This uptake might be even higher in the channel, where the dominant source, shallow soil moisture, might also be related to capillary action from the water table (see Discussion).

Risk of exposure may be particularly high for trees located in the creek channel close to the interface with the bedrock formation. These trees are likely to rely on shallow groundwater sourced from the sand-bed sediment during the dry season, an aquifer that is vulnerable to contaminated lateral subsurface inflows from the shallow bedrock. Hydraulic gradients and groundwater chemistry data strongly suggest that waters contained in the shallow bedrock flow into the riparian area during the wet season and flow recession. Further observations of isotopes and geochemistry are needed at the interface between the sand-bed sediment and bedrock aquifers to better constrain the timing and locations of inflows of bedrock groundwater into the surface water and groundwater of the riparian ecosystem.

Riparian trees along Magela Creek will be exposed to contamination via extraction of mine-derived soil water and/or groundwater. However, pot trial findings suggest that riparian woody species are unlikely to be severely impacted by $MgSO_4$ with little evidence of limitation of growth even at >1,000 mg L^{-1} $MgSO_4$. Further work is needed to refine the range of potential solute egress magnesium load from the rehabilitated landform. The estimate used here of up to 500 mg L^{-1} Mg in shallow groundwaters has a high uncertainty and a modelled value with an error estimate is needed to place pot trial findings in context of impact. Also required is further examination of the behaviour of mature vegetation at known exposure sites in situ, as findings from pot trials are only representative of the response of saplings grown in pots. High resolution remote sensing of canopy-cover change of riparian vegetation upstream and downstream of the mine at sites of known exposure may provide evidence of the impact to mature trees.

References

Ahmad M, Green DC (1986) Groundwater regimes and isotopic studies, Ranger mine area, Northern Territory. Australian Journal of Earth Sciences 33, 391-399.

Barbeta A, Burlett R, Martín-Gómez P, Fréjaville B, Devert N, Wingate L, Domec J-C, Ogée J (2020) Evidence for distinct isotopic composition of sap and tissue water in tree stems: consequences for plant water source identification. bioRxiv, 202020062018160002.

Barbeta A, Jones SP, Clavé L, Wingate L, Gimeno TE, Fréjaville B, Wohl S, Ogée J (2019) Unexplained hydrogen isotope offsets complicate the identification and quantification of tree water sources in a riparian forest. Hydrology and Earth System Sciences 23, 2129-2146.

Barbeta A, Mejía-Chang M, Ogaya R, Voltas J, Dawson TE, Peñuelas J (2015) The combined effects of a long-term experimental drought and an extreme drought on the use of plant-water sources in a Mediterranean forest. Global Change Biology 21, 1213-1225.

Begg GW, van Dam RA, Lowry JB, Finlayson CM, Walden DJ (2001) Inventory and risk assessment of water dependent ecosystems in the Daly basin, Northern Territory, Australia (Issue Supervising Scientist Report 162) Supervising Scientist.

Cakmak I, Kirkby EA (2008) Role of magnesium in carbon partitioning and alleviating photooxidative damage. Physiologia Plantarum 133, 692-704.

Canham CA, Cavalieri OY, Setterfield SA, Freestone FL, Hutley LB (2020) Effect of elevated magnesium sulfate on two riparian tree species potentially impacted by mine site contamination. Scientific Reports 10, 2880.

Canham CA, Duvert C, Beesley LS, Douglas MM, Setterfield SA, Freestone FL, Clohessy S, Loomes RC (2021) The use of regional and alluvial groundwater by riparian trees in the wet-dry tropics of northern Australia. Hydrological Processes 35, e14180.

Cartwright I, Weaver TR, Fifield LK (2006) Cl/Br ratios and environmental isotopes as indicators of recharge variability and groundwater flow: An example from the southeast Murray Basin, Australia. Chemical Geology 231, 38-56.

Chandler L, Harford AJ, Hose GC, Humphrey CL, Chariton A, Green P, Davis J (2021) Saline mine-water alters the structure and function of prokaryote communities in shallow groundwater below a tropical stream. Environmental Pollution 284, 117318.

Chen G, Auerswald K, Schnyder H (2016) ^{2}H and ^{18}O depletion of water close to organic surfaces. Biogeosciences 13, 3175-3186.

Cook PG, Hatton TJ, Pidsley D, Herczeg AL, Held A, O'Grady AP, Eamus D (1998) Water balance of a tropical woodland ecosystem, Northern Australia: a combination of micrometeorological, soil physical and groundwater chemical approaches. Journal of Hydrology 210, 161-177.

Cook PG, O'Grady AP (2006) Determining soil and ground water use of vegetation from heat pulse, water potential and stable isotope data. Oecologia 148, 97–107.

Deka RN, Wairiu M, MtakwAPW, Mullins CE, Veenendaal EM, Townend J (1995) Use and accuracy of the filter-paper technique for measurement of soil matric potential. European Journal of Soil Science 46, 233-238.

Doble R, Crosbie R, Smerdon B, Peeters L, Cook F (2012) Groundwater recharge from overbank floods. Water Resources Research 48, W09522.

Doody TM, Barron OV, Dowsley K, Emelyanova I, Fawcett J, Overton IC, Warren G (2017) Continental mapping of groundwater dependent ecosystems: A methodological framework to integrate diverse data and expert opinion. Journal of Hydrology: Regional Studies 10, 61-81.

Duvert C, Stewart MK, Cendón DI, Raiber M (2016) Time series of tritium, stable isotopes and chloride reveal short-term variations in groundwater contribution to a stream. Hydrology and Earth System Sciences 20, 257-277.

Eamus D, O'Grady AP, Hutley L (2000) Dry season conditions determine wet season water use in the wet-dry tropical savannas of northern Australia. Tree Physiology 20, 1219-1226.

Eamus D, Chen X, Kelley G, Hutley LB (2002) Root biomass and root fractal analyses of an open Eucalyptus forest in a savanna of north Australia Australian. Journal of Botany 50, 31-41.

Evaristo J, McDonnell JJ (2017) Prevalence and magnitude of groundwater use by vegetation: a global stable isotope meta-analysis. Scientific Reports 7, 44110.

Evaristo J, McDonnell JJ, Scholl MA, Bruijnzeel LA, Chun KP (2016) Insights into plant water uptake from xylem-water isotope measurements in two tropical catchments with contrasting moisture conditions. Hydrological Processes 30, 3210-3227.

Geris J, Tetzlaff D, McDonnell JJ, Soulsby C (2017) Spatial and temporal patterns of soil water storage and vegetation water use in humid northern catchments. Science of The Total Environment 595, 486-493.

Hahn M, Jacobs SR, Breuer L, Rufino MC, Windhorst D (2021) Variability in tree water uptake determined with stable water isotopes in an African tropical montane forest. Ecohydrology 14, e2278.

Harrington G, Cook P, Herczeg A (2002) Spatial and Temporal Variability of Ground Water Recharge in Central Australia: A Tracer Approach. Groundwater 40, 518-527.

Hermans C, Johnson GN, Strasser RJ, Verbruggen N (2004) Physiological characterisation of magnesium deficiency in sugar beet: acclimation to low magnesium differentially affects photosystems I and II. Planta 220, 344–355.

Hird R, Bolton MD (2017) Clarification of capillary rise in dry sand. Engineering Geology 230, 77-83.

Hutley LB, O'Grady AP, Eamus D (2000) Evapotranspiration from eucalypt open-forest savanna of northern Australia. Functional Ecology 14, 183-194 https://doiorg/101046/j1365-2435200000416x.

Kelley G (2002) Tree water use and soil water dynamics in savannas of northern Australia. PhD Thesis, Northern Territory University, https://doiorg/https://doiorg/1025913/5e7c46a02cde7.

Kelley G, O'Grady AP, Hutley LB, Eamus D (2007) A comparison of tree water use in two contiguous vegetation communities of the seasonally dry tropics of northern Australia: The

importance of site water budget to tree hydraulics. Australian Journal of Botany 55, 700-708.

Lamontagne S, Cook PG, O'Grady A, Eamus D (2005) Groundwater use by vegetation in a tropical savanna riparian zone (Daly River, Australia). Journal of Hydrology, 310, 280–293.

Leaney FW, Puhalovich AA (2006) 'Use of environmental tracers to better understand groundwater recharge/discharge processes, Ranger uranium mine, NT', CSIRO, Adelaide, SA.

Li Y, Ma Y, Song X, Wang L, Han D (2021) A δ^2H offset correction method for quantifying root water uptake of riparian trees. Journal of Hydrology 593, 125811.

Liddle DT, Boggs D, Hutley L, Yin Foo D, Boggs G, Pearson D, Cook PG, Elliott LP (2008) Biophysical modelling of water quality in a Darwin rural area groundwater dependent ecosystem. Issue NHT Project 2005/133, Northern Territory Government https://territorystoriesntgovau/10070/457657/0/0.

Liu Q, Yasufuku N, Miao J, Ren J (2014) An approach for the quick estimation of maximum height of capillary rise. Soils and Foundations 54, 1241-1245.

Malik R, Kumar S, Dahiya I (1984) An approach to quick determination of some water transmission characteristics of porous media. Soil Science 137, 395-400.

McCullough CD (2006) A multi-scale assessment of the ecological risk of magnesium sulfate to aquatic biota of Magela Creek. Northern Territory, Australia.

Munksgaard NC, Wurster CM, Bird MI (2011) Continuous analysis of $\delta^{18}O$ and δD values of water by diffusion sampling cavity ring-down spectrometry: a novel sampling device for unattended field monitoring of precipitation, ground and surface waters. Rapid Communications in Mass Spectrometry 25, 3706-3712.

O'Grady AP, Eamus D, Cook PG, Lamontagne S (2006) Comparative water use by the riparian trees Melaleuca argentea and Corymbia bella in the wet-dry tropics of northern Australia. Tree Physiology 26, 219-228.

Parnell AC, Phillips DL, Bearhop S, Semmens BX, Ward EJ, Moore JW, Jackson AL, Grey J, Kelly DJ, Inger R (2013) Bayesian stable isotope mixing models. Environmetrics 24, 387-399.

Phillips DL, Gregg JW (2003) Source partitioning using stable isotopes: coping with too many sources Oecologia 136, 261-269.

Richardson S, Irvine E, Froend R, Boon P, Barber S, Bonneville B (2011) Australian groundwater-dependent ecosystem toolbox part 1: assessment framework, Waterlines report, National Water Commission, Canberra

Sánchez-Murillo R, Birkel C (2016) Groundwater recharge mechanisms inferred from isoscapes in a complex tropical mountainous region: Tropical isoscapes. Geophysical Research Letters 43, 5060-5069.

Schreiber U, Schliwa U, Bilger W (1986) Continuous recording of photochemical and non-photochemical chlorophyll fluorescence quenching with a new type of modulation fluorometer. Photosynthesis Research 10, 51-62.

Smith GS, Johnston CM, Cornforth IS (1983) Comparison of nutrient solutions for growth of plants in sand culture. New Phytologist 94, 537-548.

Stock BC, Jackson AL, Ward EJ, Parnell AC, Phillips DL, Semmens BX (2018) Analyzing mixing systems using a new generation of Bayesian tracer mixing models. PeerJ 6, e5096.

Suckow A (2014) The age of groundwater – Definitions, models and why we do not need this term. Applied Geochemistry 50, 222-230.

Tadros CV, Hughes CE, Crawford J, Hollins SE, Chisari R (2014) Tritium in Australian precipitation: A 50 year record. Journal of Hydrology 513, 262-273.

van Dam RA, Hogan AC, McCullough CD, Houston MA, Humphrey CL, Harford AJ (2010) Aquatic toxicity of magnesium sulfate, and the influence of calcium, in very low ionic concentration water. Environmental Toxicology and Chemistry 29, 410–421.

West AG, Patrickson SJ, Ehleringer JR (2006) Water extraction times for plant and soil materials used in stable isotope analysis. Rapid Communications in Mass Spectrometry 20, 1317-1321.

Appendix 1: Pot trial statistical analyses

Table 1. One-way ANOVA analysis of Syzygium armstrongii plant height growth at final harvest.

ANOVA: Single Factor - Plant height growth (mm)

DESCRIPTION Alpha 0.05

Group	*Count*	*Sum*	*Mean*	*Variance*	*SS*	*Std Err*	*Lower*	*Upper*
5.1	6	2682	447	12590	62950	43.56901	358.5502	535.4498
69.2	6	3283	547	1989.767	9948.833	43.56901	458.7169	635.6165
467.0	6	2866	478	25901.87	129509.3	43.56901	389.2169	566.1165
961.8	6	3019	503	4724.167	23620.83	43.56901	414.7169	591.6165
1954.2	6	3162	527	16386	81930	43.56901	438.5502	615.4498
3907.2	6	3410	568	12545.07	62725.33	43.56901	479.8835	656.7831
7095.8	6	3240	540	5590	27950	43.56901	451.5502	628.4498

ANOVA

Sources	*SS*	*df*	*MS*	*F*	*P value*	*F crit*	*RMSSE*	*Omega Sq*
Between Groups	64811.29	6	10801.88	0.948403	0.47368	2.371781	0.397577	-0.00743
Within Groups	398634.3	35	11389.55					
Total	463445.6	41	11303.55					

Table 2. One-way ANOVA analysis of Syzygium armstrongii dry plant biomass at final harvest.

ANOVA: Single Factor -Dry plant biomass (g)

DESCRIPTION Alpha 0.05

Group	*Count*	*Sum*	*Mean*	*Variance*	*SS*	*Std Err*	*Lower*	*Upper*
5.1	6	192.5	32.1	63.4361	317.18	4.01962	23.9281	40.2486
69.2	6	195.4	32.6	28.7366	143.683	4.01962	24.4047	40.7253
467.0	6	159.4	26.6	148.342	741.711	4.01962	18.4081	34.7286
961.8	6	185.9	31.0	225.432	1127.16	4.01962	22.8297	39.1503
1954.2	6	208.4	34.7	84.7344	423.672	4.01962	26.5681	42.8886
3907.2	6	200.36	33.39	93.4668	467.334	4.01962	25.2331	41.5536
7095.8	6	149.6	24.9	34.4616	172.308	4.01962	16.7681	33.0886

ANOVA

Sources	*SS*	*df*	*MS*	*F*	*P value*	*F crit*	*RMSSE*	*Omega Sq*
Between Groups	476.013	6	79.3354	0.81836	0.56321	2.37178	0.36931	-0.0266
Within Groups	3393.05	35	96.9443					
Total	3869.06	41	94.3674					

Table 3. One-way ANOVA analysis of Syzygium forte plant height growth at final harvest.

ANOVA: Single Factor - Plant height growth (mm)

DESCRIPTION					Alpha	0.05		
Group	*Count*	*Sum*	*Mean*	*Variance*	*SS*	*Std Err*	*Lower*	*Upper*
5.1	6	3592	599	26317.47	131587.3	79.56694	437.1372	760.1961
69.2	6	4331	722	37734.57	188672.8	79.56694	560.3039	883.3628
467.0	6	4440	740	25888.8	129444	79.56694	578.4705	901.5295
961.8	6	3501	584	56614.3	283071.5	79.56694	421.9705	745.0295
1954.2	6	4714	786	44585.47	222927.3	79.56694	624.1372	947.1961
3907.2	6	3405	568	13792.7	68963.5	79.56694	405.9705	729.0295
7095.8	6	3696	616	60964.4	304822	79.56694	454.4705	777.5295

ANOVA

Sources	*SS*	*df*	*MS*	*F*	*P value*	*F crit*	*RMSSE*	*Omega Sq*
Between Grou	276690.5	6	46115.08	1.214022	0.322461	2.371781	0.449819	0.029667
Within Groups	1329489	35	37985.39					
Total	1606179	41	39175.1					

Table 4. One-way ANOVA analysis of Syzygium forte dry plant biomass at final harvest.

ANOVA: Single Factor - Dry plant biomass (g)

DESCRIPTION					Alpha	0.05		
Group	*Count*	*Sum*	*Mean*	*Variance*	*SS*	*Std Err*	*Lower*	*Upper*
5.1	6	232.1	38.7	45.05304	225.2652	3.090964	32.41501	44.96499
69.2	6	253.8	42.3	77.39835	386.9918	3.090964	36.03001	48.57999
467.0	6	265.3	44.2	102.8501	514.2503	3.090964	37.94168	50.49166
961.8	6	257.0	42.8	39.28414	196.4207	3.090964	36.56334	49.11332
1954.2	6	255.8	42.6	12.20212	61.0106	3.090964	36.35501	48.90499
3907.2	6	204.6	34.1	53.94419	269.7209	3.090964	27.83168	40.38166
7095.8	6	205.1	34.2	70.53867	352.6933	3.090964	27.90834	40.45832

ANOVA

Sources	*SS*	*df*	*MS*	*F*	*P value*	*F crit*	*RMSSE*	*Omega Sq*
Between Groups	649.1752	6	108.1959	1.887432	0.11071	2.371781	0.560867	0.112512
Within Groups	2006.353	35	57.32437					
Total	2655.528	41	64.76898					

Table 5. One-way ANOVA analysis of Lophopetalum arnhemicum plant height growth at final harvest.

ANOVA: Single Factor - Plant height growth (mm)

DESCRIPTION					Alpha	0.05		
Group	*Count*	*Sum*	*Mean*	*Variance*	*SS*	*Std Err*	*Lower*	*Upper*
5.1	6	1640	273	8602.267	43011.33	43.10544	185.8246	360.842
69.2	6	1706	284	7531.467	37657.33	43.10544	196.8246	371.842
467.0	6	1818	303	7211.6	36058	43.10544	215.4913	390.5087
961.8	6	2071	345	19066.97	95334.83	43.10544	257.658	432.6754
1954.2	6	1823	304	5553.767	27768.83	43.10544	216.3246	391.342
3907.2	6	2282	380	24034.27	120171.3	43.10544	292.8246	467.842
7095.8	6	2083	347	6038.967	30194.83	43.10544	259.658	434.6754

ANOVA

Sources	*SS*	*df*	*MS*	*F*	*P value*	*F crit*	*RMSSE*	*Omega Sq*
Between Groups	54063.62	6	9010.603	0.808237	0.570542	2.371781	0.367023	-0.02817
Within Groups	390196.5	35	11148.47					
Total	444260.1	41	10835.61					

Table 6. One-way ANOVA analysis of Lophopetalum arnhemicum dry plant biomass at final harvest.

ANOVA: Single Factor - Dry plant biomass (g)

DESCRIPTION					Alpha	0.05		
Group	*Count*	*Sum*	*Mean*	*Variance*	*SS*	*Std Err*	*Lower*	*Upper*
5.1	6	110.7	18.4	47.77322	238.8661	2.288558	13.79565	23.08769
69.2	6	109.55	18.26	11.64314	58.21568	2.288558	13.61231	22.90435
467.0	6	118.62	19.77	20.31088	101.5544	2.288558	15.12398	24.41602
961.8	6	127.40	21.23	36.58279	182.9139	2.288558	16.58731	25.87935
1954.2	6	115.25	19.21	56.99782	284.9891	2.288558	14.56231	23.85435
3907.2	6	101.59	16.93	21.85838	109.2919	2.288558	12.28565	21.57769
7095.8	6	93.40	15.57	24.80875	124.0437	2.288558	10.92065	20.21269

ANOVA

Sources	*SS*	*df*	*MS*	*F*	*P value*	*F crit*	*RMSSE*	*Omega Sq*
Between Groups	124.2631	6	20.71051	0.659046	0.682803	2.371781	0.331423	-0.0512
Within Groups	1099.875	35	31.42499					
Total	1224.138	41	29.85702					

Table 7. One-way ANOVA analysis of Carallia brachiata plant height growth at final harvest.

ANOVA: Single Factor - Plant height growth (mm)

DESCRIPTION					Alpha	0.05		
Group	*Count*	*Sum*	*Mean*	*Variance*	*SS*	*Std Err*	*Lower*	*Upper*
5.1	6	838	140	2462.27	12311.3	20.9961	97.0423	182.291
69.2	6	1274	212	5197.07	25985.3	20.9961	169.709	254.9577
467.0	6	774	129	1185.2	5926	20.9961	86.3756	171.6244
961.8	6	758	126	1428.27	7141.33	20.9961	83.709	168.9577
1954.2	6	900	150	1894	9470	20.9961	107.376	192.6244
3907.2	6	947	158	3706.97	18534.8	20.9961	115.209	200.4577
7095.8	6	757	126	2641.37	13206.8	20.9961	83.5423	168.791

ANOVA								
Sources	*SS*	*df*	*MS*	*F*	*P value*	*F crit*	*RMSSE*	*Omega Sq*
Between Groups	33672	6	5611.99	2.12172	0.0754	2.37178	0.59466	0.138114
Within Groups	92575.7	35	2645.02					
Total	126248	41	3079.21					

Table 8. One-way ANOVA analysis of Carallia brachiata dry plant biomass at final harvest.

ANOVA: Single Factor - Dry plant biomass (g)

DESCRIPTION					Alpha	0.05		
Group	*Count*	*Sum*	*Mean*	*Variance*	*SS*	*Std Err*	*Lower*	*Upper*
5.1	6	75.0	12.5	41.14495	205.7247	3.823866	4.743806	20.26953
69.2	6	136.3	22.7	80.22631	401.1315	3.823866	14.95381	30.47953
467.0	6	54.8	9.1	73.64507	368.2254	3.823866	1.362139	16.88786
961.8	6	104.8	17.5	185.7791	928.8957	3.823866	9.710473	25.23619
1954.2	6	98.5	16.4	91.98871	459.9435	3.823866	8.653806	24.17953
3907.2	6	70.7	11.8	58.0846	290.423	3.823866	4.027139	19.55286
7095.8	6	81.5	13.6	83.25319	416.2659	3.823866	5.820473	21.34619

ANOVA								
Sources	*SS*	*df*	*MS*	*F*	*P value*	*F crit*	*RMSSE*	*Omega Sq*
Between Groups	722.6358	6	120.4393	1.372814	0.252761	2.371781	0.478333	0.050566
Within Groups	3070.61	35	87.73171					
Total	3793.246	41	92.51818					

Table 9. One-way ANOVA analysis and Tukey HSD test of Pandanus aquaticus plant height growth at final harvest.

ANOVA: Single Factor - Plant height growth (mm)

DESCRIPTION					Alpha	0.05		
Group	*Count*	*Sum*	*Mean*	*Variance*	*SS*	*Std Err*	*Lower*	*Upper*
5.1	6	3364	560.7	5302.3	26511.3333	28.2753	503.265	618.069
69.2	6	3468	578.0	3109.6	15548	28.2753	520.598	635.402
467.0	6	3165	527.5	6664.7	33323.5	28.2753	470.098	584.902
961.8	6	3331	555.2	1195.8	5978.83333	28.2753	497.765	612.569
1954.2	6	3786	631.0	3190.8	15954	28.2753	573.598	688.402
3907.2	6	4473	745.5	4333.5	21667.5	28.2753	688.098	802.902
7095.8	6	4373	728.8	9782.2	48910.8333	28.2753	671.431	786.235

ANOVA

Sources	*SS*	*df*	*MS*	*F*	*P value*	*Eta-sq*	*RMSSE*	*Omega Sq*
Between Group	274408	6	45734.6	9.53406	3.2228E-06	0.62041	1.26056	0.54938
Within Groups	167894	35	4796.97					
Total	442302	41	10787.8					

TUKEY HSD/KRAMER		alpha	0.05		
group	*mean*	*n*	*ss*	*df*	*q-crit*
5.1	560.7	6	26511.3		
69.2	578.0	6	15548		
467.0	527.5	6	33323.5		
961.8	555.2	6	5978.83		
1954.2	631.0	6	15954		
3907.2	745.5	6	21667.5		
7095.8	728.8	6	48910.8		
		42	167894	35	4.421

Q TEST

group 1	*group 2*	*mean*	*std err*	*q-stat*	*lower*	*upper*	*p-value*	*mean-crit*	*Cohen d*
5.1	69.2	17.3333	28.2753	0.61302	-107.67	142.339	0.999420286	125.005	0.25026
5.1	467.0	33.1667	28.2753	1.17299	-91.839	158.172	0.98010369	125.005	0.47887
5.1	961.8	5.5	28.2753	0.19452	-119.51	130.505	0.999999329	125.005	0.07941
5.1	1954.2	70.3333	28.2753	2.48744	-54.672	195.339	0.583047536	125.005	1.01549
5.1	3907.2	184.833	28.2753	6.53691	59.828	309.839	0.000903897	125.005	2.66868
5.1	7095.8	168.167	28.2753	5.94747	43.1614	293.172	0.002975982	125.005	2.42804
69.2	467.0	50.5	28.2753	1.78601	-74.505	175.505	0.863808282	125.005	0.72913
69.2	961.8	22.8333	28.2753	0.80754	-102.17	147.839	0.997261551	125.005	0.32967
69.2	1954.2	53	28.2753	1.87442	-72.005	178.005	0.83543672	125.005	0.76523
69.2	3907.2	167.5	28.2753	5.92389	42.4947	292.505	0.00311862	125.005	2.41842
69.2	7095.8	150.833	28.2753	5.33445	25.828	275.839	0.009780917	125.005	2.17778
467.0	961.8	27.6667	28.2753	0.97847	-97.339	152.672	0.992233655	125.005	0.39946
467.0	1954.2	103.5	28.2753	3.66043	-21.505	228.505	0.160588239	125.005	1.49437
467.0	3907.2	218	28.2753	7.7099	92.9947	343.005	7.79614E-05	125.005	3.14755
467.0	7095.8	201.333	28.2753	7.12045	76.328	326.339	0.000269535	125.005	2.90691
961.8	1954.2	75.8333	28.2753	2.68196	-49.172	200.839	0.495940987	125.005	1.09491
961.8	3907.2	190.333	28.2753	6.73142	65.328	315.339	0.000605509	125.005	2.74809
961.8	7095.8	173.667	28.2753	6.14198	48.6614	298.672	0.002017034	125.005	2.50745
1954.2	3907.2	114.5	28.2753	4.04946	-10.505	239.505	0.090740698	125.005	1.65319
1954.2	7095.8	97.8333	28.2753	3.46002	-27.172	222.839	0.210262211	125.005	1.41255
3907.2	7095.8	16.6667	28.2753	0.58944	-108.34	141.672	0.999537031	125.005	0.24064

Table 10. One-way ANOVA analysis and Tukey HSD test of Pandanus aquaticus dry plant biomass at final harvest.

ANOVA: Single Factor - Dry plant biomass (g)

DESCRIPTION Alpha 0.05

Group	*Count*	*Sum*	*Mean*	*Variance*	*SS*	*Std Err*	*Lower*	*Upper*
5.1	6	261.4	43.6	33.689	168.4470833	1.88591	39.7297	47.3869
69.2	6	274.4	45.7	30.824	154.1177333	1.88591	41.9081	49.5653
467.0	6	233.5	38.9	15.237	76.18673333	1.88591	35.0947	42.7519
961.8	6	278.1	46.4	18.379	91.89748333	1.88591	42.5231	50.1803
1954.2	6	294.9	49.2	8.9541	44.77035	1.88591	45.3264	52.9836
3907.2	6	333.1	55.5	27.706	138.5292833	1.88591	51.6897	59.3469
7095.8	6	310.2	51.7	14.589	72.94613333	1.88591	47.8681	55.5253

ANOVA

Sources	*SS*	*df*	*MS*	*F*	*P value*	*Eta-sq*	*RMSSE*	*Omega Sq*
Between Groups	1066.93	6	177.821	8.3328	1.21527E-05	0.58822	1.17847	0.51161
Within Groups	746.895	35	21.3399					
Total	1813.82	41	44.2395					

TUKEY HSD/KRAMER alpha 0.05

group	*mean*	*n*	*ss*	*df*	*q-crit*
5.1	43.6	6	168.447		
69.2	45.7	6	154.118		
467.0	38.9	6	76.1867		
961.8	46.4	6	91.8975		
1954.2	49.2	6	44.7704		
3907.2	55.5	6	138.529		
7095.8	51.7	6	72.9461		
		42	746.895	35	4.421

Q TEST

group 1	*group 2*	*mean*	*std err*	*q-stat*	*lower*	*upper*	*p-value*	*mean-crit*	*Cohen d*
5.1	69.2	2.17833	1.88591	1.15506	-6.1593	10.5159	0.981594789	8.33759	0.47155
5.1	467.0	4.635	1.88591	2.4577	-3.7026	12.9726	0.596455846	8.33759	1.00335
5.1	961.8	2.79333	1.88591	1.48116	-5.5443	11.1309	0.938901283	8.33759	0.60468
5.1	1954.2	5.59667	1.88591	2.96763	-2.7409	13.9343	0.375752665	8.33759	1.21153
5.1	3907.2	11.96	1.88591	6.34178	3.62241	20.2976	0.001346531	8.33759	2.58902
5.1	7095.8	8.13833	1.88591	4.31534	-0.1993	16.4759	0.059490034	8.33759	1.76173
69.2	467.0	6.81333	1.88591	3.61276	-1.5243	15.1509	0.171494843	8.33759	1.4749
69.2	961.8	0.615	1.88591	0.3261	-7.7226	8.95259	0.999985481	8.33759	0.13313
69.2	1954.2	3.41833	1.88591	1.81257	-4.9193	11.7559	0.85558159	8.33759	0.73998
69.2	3907.2	9.78167	1.88591	5.18672	1.44408	18.1193	0.012901253	8.33759	2.11747
69.2	7095.8	5.96	1.88591	3.16028	-2.3776	14.2976	0.30381606	8.33759	1.29018
467.0	961.8	7.42833	1.88591	3.93887	-0.9093	15.7659	0.107369123	8.33759	1.60804
467.0	1954.2	10.2317	1.88591	5.42533	1.89408	18.5693	0.008231706	8.33759	2.21488
467.0	3907.2	16.595	1.88591	8.79948	8.25741	24.9326	7.74328E-06	8.33759	3.59237
467.0	7095.8	12.7733	1.88591	6.77305	4.43574	21.1109	0.000555545	8.33759	2.76509
961.8	1954.2	2.80333	1.88591	1.48646	-5.5343	11.1409	0.937901923	8.33759	0.60685
961.8	3907.2	9.16667	1.88591	4.86062	0.82908	17.5043	0.023383843	8.33759	1.98434
961.8	7095.8	5.345	1.88591	2.83418	-2.9926	13.6826	0.430233549	8.33759	1.15705
1954.2	3907.2	6.36333	1.88591	3.37415	-1.9743	14.7009	0.234685289	8.33759	1.37749
1954.2	7095.8	2.54167	1.88591	1.34772	-5.7959	10.8793	0.960647723	8.33759	0.5502
3907.2	7095.8	3.82167	1.88591	2.02644	-4.5159	12.1593	0.780526309	8.33759	0.82729

Table 11. One-way ANOVA analysis of Barringtonia acutangula plant height growth at final harvest.

ANOVA: Single Factor - Plant height growth (mm)

DESCRIPTION					Alpha	0.05		
Group	*Count*	*Sum*	*Mean*	*Variance*	*SS*	*Std Err*	*Lower*	*Upper*
5.1	6	146.70	24.45	9.84836	49.2418	1.04867	22.3209	26.5787
69.2	6	145.17	24.20	9.11727	45.5864	1.04867	22.0662	26.324
467.0	6	156.79	26.13	6.3544	31.772	1.04867	24.0029	28.2607
961.8	6	156.43	26.07	5.07898	25.3949	1.04867	23.9434	28.2013
1954.2	6	137.93	22.99	3.88971	19.4486	1.04867	20.8586	25.1164
3907.2	6	153.18	25.53	2.69199	13.46	1.04867	23.4006	27.6584
7095.8	6	142.18	23.70	9.20744	46.0372	1.04867	21.5669	25.8248

ANOVA

Sources	*SS*	*df*	*MS*	*F*	*P value*	*Eta-sq*	*RMSSE*	*Omega Sq*
Between	53.2576	6	8.87627	1.34523	0.26383	0.1874	0.4735	0.047
Within Gr	230.941	35	6.59831					
Total	284.198	41	6.93167					

Table 12. One-way ANOVA analysis of Barringtonia acutangula dry plant biomass at final harvest.

ANOVA: Single Factor - Dry plant biomass (g)

DESCRIPTION					Alpha	0.05		
Group	*Count*	*Sum*	*Mean*	*Variance*	*SS*	*Std Err*	*Lower*	*Upper*
5.1	6	106.3	17.7	27.7373	138.687	1.77031	14.1194	21.3073
69.2	6	127.5	21.2	20.8325	104.162	1.77031	17.6511	24.8389
467.0	6	130.0	21.7	17.9487	89.7437	1.77031	18.0794	25.2673
961.8	6	118.2	19.7	36.4343	182.172	1.77031	16.1127	23.3006
1954.2	6	111.0	18.5	15.8336	79.1682	1.77031	14.9111	22.0989
3907.2	6	99.5	16.6	2.66863	13.3431	1.77031	12.9927	20.1806
7095.8	6	113.3	18.9	10.1728	50.8638	1.77031	15.2861	22.4739

ANOVA

Sources	*SS*	*df*	*MS*	*F*	*P value*	*Eta-sq*	*RMSSE*	*Omega Sq*
Between Groups	121.08	6	20.1801	1.07318	0.39711	0.15539	0.42292	0.01035
Within Groups	658.139	35	18.804					
Total	779.22	41	19.0054					

Table 13. One-way ANOVA analysis of Alphitonia excelsa plant height growth at final harvest.

ANOVA: Single Factor -Plant height growth (mm)

DESCRIPTION					Alpha	0.05		
Group	*Count*	*Sum*	*Mean*	*Variance*	*SS*	*Std Err*	*Lower*	*Upper*
5.1	6	137.86	22.98	5.66039	28.302	1.53001	19.8525	26.10185
69.2	6	134.76	22.46	12.8735	64.3676	1.53001	19.335	25.58441
467.0	6	126.61	21.10	14.0253	70.1267	1.53001	17.9777	24.22711
961.8	6	112.68	18.78	13.9648	69.8238	1.53001	15.6555	21.90489
1954.2	6	133.65	22.28	14.167	70.8348	1.53001	19.1507	25.40011
3907.2	6	121.10	20.18	23.5822	117.911	1.53001	17.0582	23.30756

ANOVA

Sources	*SS*	*df*	*MS*	*F*	*P value*	*Eta-sq*	*RMSSE*	*Omega Sq*
Between	76.4732	5	15.2946	1.08893	0.38668	0.15361	0.42602	0.012201
Within Gr	421.366	30	14.0455					
Total	497.839	35	14.224					

Table 14. One-way ANOVA analysis of Alphitonia excelsa dry plant biomass at final harvest.

ANOVA: Single Factor - Dry plant biomass (g)

DESCRIPTION					Alpha	0.05		
Group	*Count*	*Sum*	*Mean*	*Variance*	*SS*	*Std Err*	*Lower*	*Upper*
5.1	6	28.33	4.72	0.77021	3.85104	0.35517	3.99691	5.44763
69.2	6	26.93	4.49	0.13925	0.69624	0.35517	3.7634	5.21412
467.0	6	31.51	5.25	0.68457	3.42285	0.35517	4.52595	5.97666
961.8	6	27.76	4.63	0.87412	4.37059	0.35517	3.90209	5.3528
1954.2	6	27.53	4.59	1.0694	5.34699	0.35517	3.86218	5.3129
3907.2	6	31.61	5.27	1.00376	5.01878	0.35517	4.54375	5.99447

ANOVA

Sources	*SS*	*df*	*MS*	*F*	*P value*	*Eta-sq*	*RMSSE*	*Omega Sq*
Between Groups	3.58798	5	0.7176	0.94809	0.46471	0.13645	0.39751	-0.0073
Within Groups	22.7065	30	0.75688					
Total	26.2945	35	0.75127					

Table 15. One factor PERMANOVA analysis of mean plant height to biomass (H/B) ratio of Syzygium armstrongii at final harvest.

PERMANOVA
Permutational MANOVA

Resemblance worksheet
Name: Resem2
Data type: Distance
Selection: All
Resemblance: D1 Euclidean distance

Sums of squares type: Type III (partial)
Fixed effects sum to zero for mixed terms
Permutation method: Unrestricted permutation of raw data
Number of permutations: 999

Factors

Name	Abbrev.	Type	Levels
Treatment	Tr	Fixed	7

PERMANOVA table of results

Source	df	SS	MS	Pseudo-F	P(perm)	Unique perms
Tr	6	967.05	161.18	0.70019	0.726	999
Res	35	8056.6	230.19			
Total	41	9023.7				

Details of the expected mean squares (EMS) for the model

Source	EMS
Tr	1*V(Res) + 6*S(Tr)
Res	1*V(Res)

Construction of Pseudo-F ratio(s) from mean squares

Source	Numerato	Denomina	Num.df	Den.df
Tr	1*Tr	1*Res	6	35

Estimates of components of variation

Source	Estimate	Sq.root
S(Tr)	-11.502	-3.3915
V(Res)	230.19	15.172

Table 16. One factor PERMANOVA analysis of mean plant height to biomass (H/B) ratio of Syzygium forte at final harvest.

PERMANOVA
Permutational MANOVA

Resemblance worksheet
Name: Resem2
Data type: Distance
Selection: All
Resemblance: D1 Euclidean distance

Sums of squares type: Type III (partial)
Fixed effects sum to zero for mixed terms
Permutation method: Unrestricted permutation of raw data
Number of permutations: 999

Factors

Name	Abbrev.	Type	Levels
Treatment	Tr	Fixed	7

PERMANOVA table of results

Source	df	SS	MS	Pseudo-F	P(perm)	Unique perms
Tr	6	263.71	43.951	2.0151	0.07	998
Res	35	763.37	21.811			
Total	41	1027.1				

Details of the expected mean squares (EMS) for the model

Source	EMS
Tr	1*V(Res) + 6*S(Tr)
Res	1*V(Res)

Construction of Pseudo-F ratio(s) from mean squares

Source	Numerator	Denominator	Num.df	Den.df
Tr	1*Tr	1*Res	6	35

Estimates of components of variation

Source	Estimate	Sq.root
S(Tr)	3.6901	1.921
V(Res)	21.811	4.6702

Table 17. One factor PERMANOVA analysis of mean plant height to biomass (H/B) ratio of Lophopetalum arnhemicum at final harvest.

PERMANOVA
Permutational MANOVA

Resemblance worksheet
Name: Resem2
Data type: Distance
Selection: All
Resemblance: D1 Euclidean distance

Sums of squares type: Type III (partial)
Fixed effects sum to zero for mixed terms
Permutation method: Unrestricted permutation of raw data
Number of permutations: 999

Factors

Name	Abbrev.	Type	Levels
Treatment	Tr	Fixed	7

PERMANOVA table of results

Source	df	SS	MS	Pseudo-F	P(perm)	Unique perms
Tr	6	639.18	106.53	0.87031	0.56	998
Res	35	4284.1	122.4			
Total	41	4923.3				

Details of the expected mean squares (EMS) for the model

Source	EMS
Tr	1*V(Res) + 6*S(Tr)
Res	1*V(Res)

Construction of Pseudo-F ratio(s) from mean squares

Source	Numerato	Denomina	Num.df	Den.df
Tr	1*Tr	1*Res	6	35

Estimates of components of variation

Source	Estimate	Sq.root
S(Tr)	-2.6457	-1.6266
V(Res)	122.4	11.064

Table 18. One factor PERMANOVA analysis of mean plant height to biomass (H/B) ratio of Carallia brachiata at final harvest.

PERMANOVA
Permutational MANOVA

Resemblance worksheet
Name: Resem2
Data type: Distance
Selection: All
Resemblance: D1 Euclidean distance

Sums of squares type: Type III (partial)
Fixed effects sum to zero for mixed terms
Permutation method: Unrestricted permutation of raw data
Number of permutations: 999

Factors

Name	Abbrev.	Type	Levels
Treatment	Tr	Fixed	7

PERMANOVA table of results

Source	df	SS	MS	Pseudo-F	P(perm)	Unique perms
Tr	6	738.65	123.11	1.179	0.36	999
Res	35	3654.6	104.42			
Total	41	4393.3				

Details of the expected mean squares (EMS) for the model

Source	EMS
Tr	1*V(Res) + 6*S(Tr)
Res	1*V(Res)

Construction of Pseudo-F ratio(s) from mean squares

Source	Numerato	Denomina	Num.df	Den.df
Tr	1*Tr	1*Res	6	35

Estimates of components of variation

Source	Estimate	Sq.root
S(Tr)	3.115	1.7649
V(Res)	104.42	10.218

Table 19. One factor PERMANOVA analysis and pairwise tests of mean plant height to biomass (H/B) ratio of Pandanus aquaticus at final harvest.

PERMANOVA
Permutational MANOVA

Resemblance worksheet
Name: Resem2
Data type: Distance
Selection: All
Resemblance: D1 Euclidean distance

Sums of squares type: Type III (partial)
Fixed effects sum to zero for mixed terms
Permutation method: Unrestricted permutation of raw data
Number of permutations: 999

Factors

Name	Abbrev.	Type	Levels
Treatment	Tr	Fixed	7

PERMANOVA table of results

Source	df	SS	MS	Pseudo-F	P(perm)	Unique perms
Tr	6	183.79	30.632	12.3	0.001	999
Res	35	87.164	2.4904			
Total	41	270.96				

Details of the expected mean squares (EMS) for the model

Source	EMS
Tr	1*V(Res) + 6*S(Tr)
Res	1*V(Res)

Construction of Pseudo-F ratio(s) from mean squares

Source	Numerato	Denomina	Num.df	Den.df
Tr	1*Tr	1*Res	6	35

Estimates of components of variation

Source	Estimate	Sq.root
S(Tr)	4.6903	2.1657
V(Res)	2.4904	1.5781

PAIR-WISE TESTS

Term 'Tr'

Groups	t	P(perm)	Unique perms
T1, T2	0.92644	0.36	408
T1, T3	2.4139	0.016	411
T1, T4	3.609	0.003	409
T1, T5	4.5398	0.004	411
T1, T6	6.9406	0.004	400
T1, T7	5.7078	0.005	394
T2, T3	1.2058	0.239	394
T2, T4	2.0821	0.061	402
T2, T5	2.8927	0.001	395
T2, T6	4.463	0.001	412
T2, T7	4.3016	0.002	408
T3, T4	2.2877	0.046	404
T3, T5	2.6558	0.003	412
T3, T6	4.9112	0.005	412
T3, T7	4.0521	0.004	408
T4, T5	1.6207	0.112	399
T4, T6	3.9179	0.002	413
T4, T7	3.6382	0.007	406
T5, T6	1.7943	0.061	404
T5, T7	2.3295	0.026	420
T6, T7	1.3857	0.18	400

Table 20. One factor PERMANOVA analysis of mean plant height to biomass (H/B) ratio of Barringtonia acutangula at final harvest.

PERMANOVA
Permutational MANOVA

Resemblance worksheet
Name: Resem2
Data type: Distance
Selection: All
Resemblance: D1 Euclidean distance

Sums of squares type: Type III (partial)
Fixed effects sum to zero for mixed terms
Permutation method: Unrestricted permutation of raw data
Number of permutations: 999

Factors

Name	Abbrev.	Type	Levels
Treatment	Tr	Fixed	7

PERMANOVA table of results

Source	df	SS	MS	Pseudo-F	P(perm)	Unique perms
Tr	6	870.08	145.01	1.9723	0.098	998
Res	35	2573.4	73.524			
Total	41	3443.4				

Details of the expected mean squares (EMS) for the model

Source	EMS
Tr	1*V(Res) + 6*S(Tr)
Res	1*V(Res)

Construction of Pseudo-F ratio(s) from mean squares

Source	Numerato	Denomina	Num.df	Den.df
Tr	1*Tr	1*Res	6	35

Estimates of components of variation

Source	Estimate	Sq.root
S(Tr)	11.915	3.4518
V(Res)	73.524	8.5746

Table 21. One factor PERMANOVA analysis and pairwise tests of mean plant height to biomass (H/B) ratio of Alphitonia excelsa at final harvest.

PERMANOVA
Permutational MANOVA

Resemblance worksheet
Name: Resem2
Data type: Distance
Selection: All
Resemblance: D1 Euclidean distance

Sums of squares type: Type III (partial)
Fixed effects sum to zero for mixed terms
Permutation method: Unrestricted permutation of raw data
Number of permutations: 999

Factors

Name	Abbrev.	Type	Levels
Treatment	Tr	Fixed	6

PERMANOVA table of results

Source	df	SS	MS	Pseudo-F	P(perm)	Unique perms
Tr	5	829.92	165.98	3.2134	0.018	998
Res	30	1549.6	51.654			
Total	35	2379.5				

Details of the expected mean squares (EMS) for the model

Source	EMS
Tr	1*V(Res) + 6*S(Tr)
Res	1*V(Res)

Construction of Pseudo-F ratio(s) from mean squares

Source	Numerato	Denomina	Num.df	Den.df
Tr	1*Tr	1*Res	5	30

Estimates of components of variation

Source	Estimate	Sq.root
S(Tr)	19.055	4.3652
V(Res)	51.654	7.1871

PAIR-WISE TESTS

Term 'Tr'

Groups	t	P(perm)	Unique perms
T1, T2	0.40043	0.730	414
T1, T3	2.7008	0.028	414
T1, T4	2.369	0.041	408
T1, T5	0.97066	0.335	413
T1, T6	2.7184	0.017	413
T2, T3	2.165	0.044	400
T2, T4	1.9564	0.073	404
T2, T5	0.60602	0.558	405
T2, T6	2.2656	0.052	415
T3, T4	0.41446	0.665	405
T3, T5	2.2667	0.036	398
T3, T6	0.89436	0.403	413
T4, T5	1.9258	0.089	398
T4, T6	0.70065	0.526	406
T5, T6	2.141	0.068	410

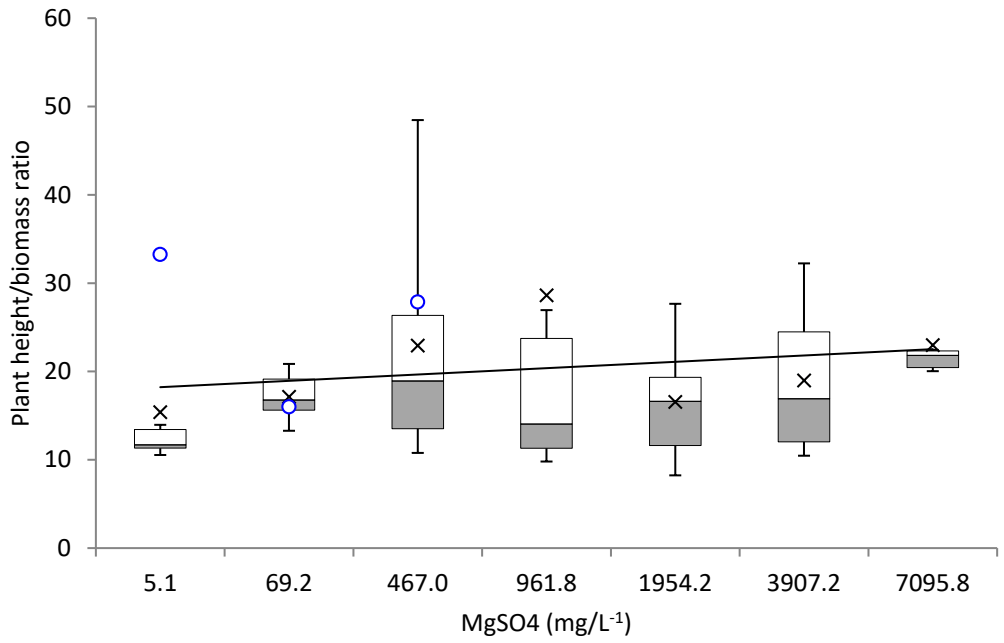

Figure 1. Mean plant height to biomass ratio and $MgSO_4$ treatment concentrations for Syzygium armstrongii.

Table 22. Regression analysis for mean plant height to biomass ratio and $MgSO_4$ treatment concentrations for Syzygium armstrongii.

Regression Analysis

OVERALL FIT	
Multiple R	0.197555
R Square	0.039028
Adjusted R	-0.15317
Standard E	2797.261
Observatic	7

AIC	112.7542
AICc	120.7542
SBC	112.6461

ANOVA					Alpha	0.05
	df	*SS*	*MS*	*F*	*p-value*	*sig*
Regressior	1	1588913	1588913	0.203065	0.671127	no
Residual	5	39123336	7824667			
Total	6	40712249				

	coeff	*std err*	*t stat*	*p-value*	*lower*	*upper*
Intercept	-159.628	5050.324	-0.03161	0.976008	-13141.9	12822.64
Mean	109.2291	242.3936	0.450627	0.671127	-513.863	732.3216

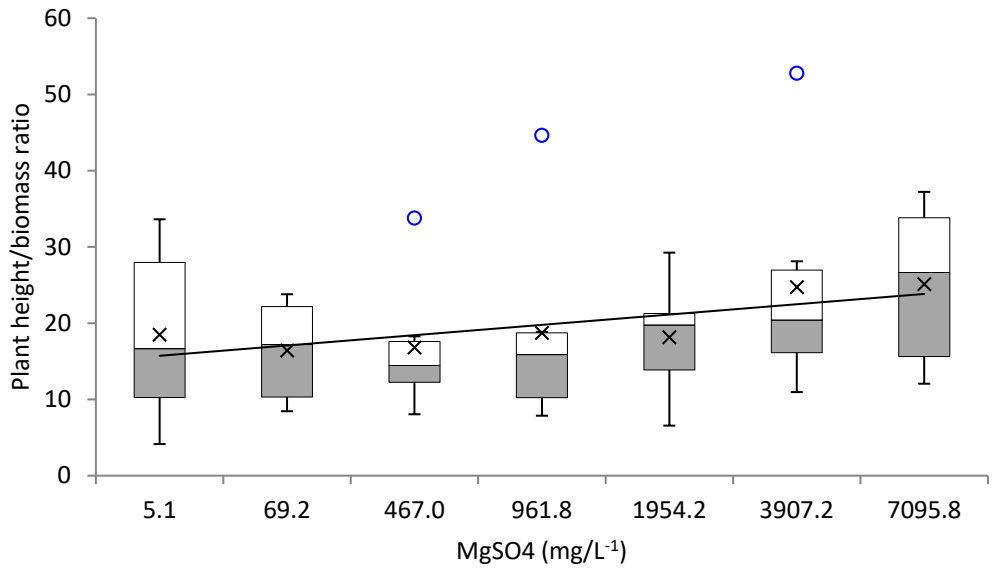

Figure 2. Mean plant height to biomass ratio and $MgSO_4$ treatment concentrations for Lophopetalum arnhemicum.

Table 23. Regression analysis for mean plant height to biomass ratio and $MgSO_4$ treatment concentrations for Lophopetalum arnhemicum.

Regression Analysis

OVERALL FIT	
Multiple R	0.909822
R Square	0.827776
Adjusted R Squar	0.793331
Standard Error	1184.199
Observations	7

AIC	100.7202
AICc	108.7202
SBC	100.612

ANOVA					Alpha	0.05
	df	*SS*	*MS*	*F*	*p-value*	*sig*
Regression	1	33700609	33700609	24.0319	0.004466	yes
Residual	5	7011640	1402328			
Total	6	40712249				

	coeff	*std err*	*t stat*	*p-value*	*lower*	*upper*
Intercept	-10891.4	2680.734	-4.06283	0.009702	-17782.4	-4000.32
Mean	655.0908	133.6311	4.902234	0.004466	311.5812	998.6004

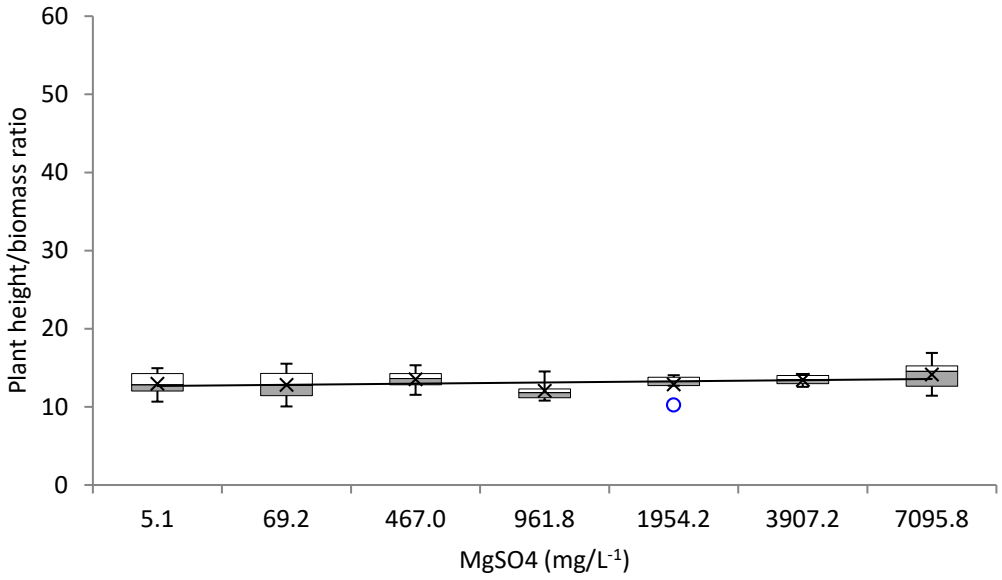

Figure 3. Mean plant height to biomass ratio and $MgSO_4$ treatment concentrations for Pandanus aquaticus.

Table 24. Regression analysis for mean plant height to biomass ratio and $MgSO_4$ treatment concentrations for Pandanus aquaticus.

Regression Analysis

OVERALL FIT	
Multiple R	0.701435
R Square	0.492012
Adjusted R Squa	0.390414
Standard Error	2033.782
Observations	7

AIC	108.2918
AICc	116.2918
SBC	108.1836

ANOVA					Alpha	0.05
	df	*SS*	*MS*	*F*	*p-value*	*sig*
Regression	1	20030897	20030897	4.842744	0.079032	no
Residual	5	20681351	4136270			
Total	6	40712249				

	coeff	*std err*	*t stat*	*p-value*	*lower*	*upper*
Intercept	-34131.1	16466.39	-2.07277	0.092912	-76459.3	8197.14
Mean	2758.593	1253.55	2.200624	0.079032	-463.761	5980.946

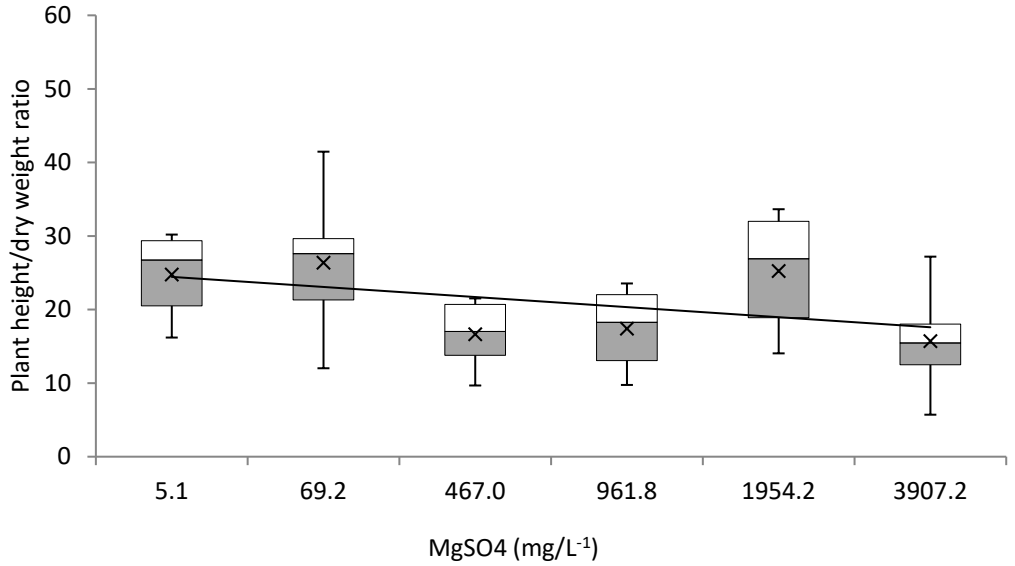

Figure 4. Mean plant height to biomass ratio and $MgSO_4$ treatment concentrations for Alphitonia excelsa.

Table 25. Regression analysis for mean plant height to biomass ratio and $MgSO_4$ treatment concentrations for Alphitonia excelsa.

Regression Analysis

OVERALL FIT			
Multiple R	0.480622	AIC	89.058741
R Square	0.230997	AICc	101.05874
Adjusted R Square	0.038747	SBC	88.64226
Standard Error	1466.98		
Observations	6		

ANOVA					Alpha	0.05
	df	*SS*	*MS*	*F*	*p-value*	*sig*
Regression	1	2585757	2585757	1.2015435	0.334578	no
Residual	4	8608118	2152030			
Total	5	11193875				

	coeff	*std err*	*t stat*	*p-value*	*lower*	*upper*
Intercept	4302.417	2868.494	1.499887	0.2080278	-3661.8	12266.63
Mean	-146.293	133.4613	-1.09615	0.3345783	-516.841	224.2544

Appendix 2: Pot trial root mass photographs

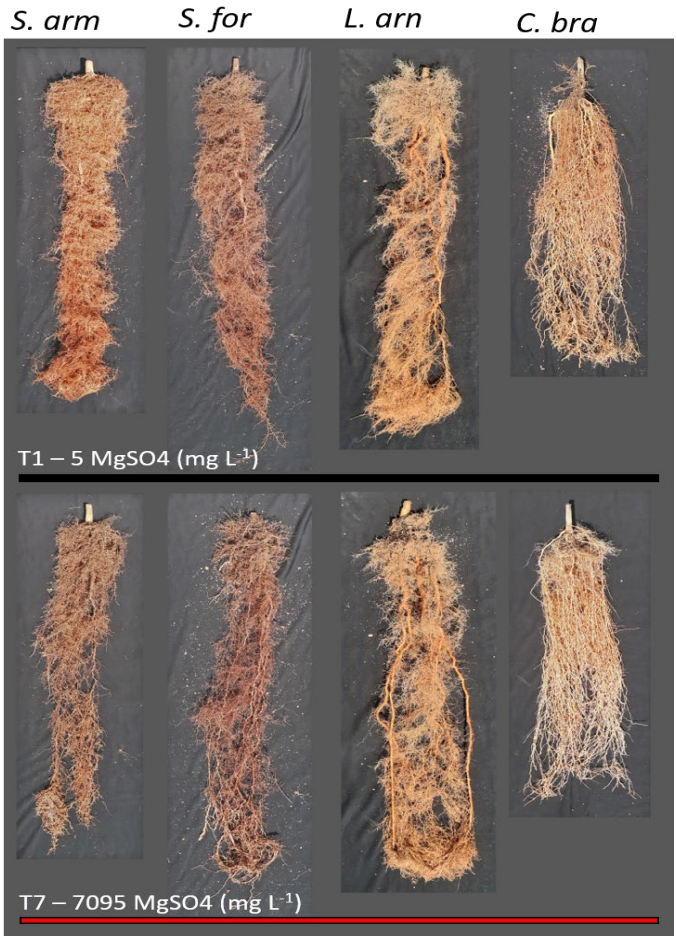

Figure 1. Examples of T1 (Control, upper panels) and T7 (lower panels) root mass from phase II pot trial species Syzygium armstrongii, Syzygium forte, Lophopetalum arnhemicum and Carallia brachiata at harvest. No obvious differences in root morphology (mass, density, colour) were evident among the four species.

Pandanus aquaticus

Figure 2. Root mass of all six replicate plants of phase III pot trial species Pandanus aquaticus from the T1 (Control, upper panels) and T7 (lower panels) treatments at harvest. A marked difference in root density and morphology was evident between treatments, with T7 plants generally having lower mass with fewer fibrous root hairs.

Barringtonia acutangula

Figure 3. Root growth of all six replicate plants of phase III pot trial species Barringtonia acutangula from the T1 (Control, upper panels) and T7 (lower panels) treatments. No obvious differences in root morphology were evident between treatments.

Alphitonia excelsa

Figure 4. Root growth of all six replicate plants of phase III pot trial species Alphitonia excelsa from the T1 (Control, upper panels) and T6 (lower panels) treatments. Although no obvious morphological differences were evident between treatments, colouration of roots in the T6 treatment appeared slightly darker than control T1 plants.

Appendix 3: Stable isotope data

Table 1. Isotope and electrical conductivity data for the sand-bed and bedrock aquifers.

Bore or piezometer	Groundwater unit	Corresponding site	Screen depth	$\delta^{18}O$ (‰)	δD (‰)	Conductivity (µS/cm)
MCP07	sand-bed	MC3	<2 m	-4.57	-27.27	52.0
MCP08	sand-bed	MC3	<2 m	-3.36	-20.18	140.0
MCP08	sand-bed	MC3	<2 m	-3.06	-18.37	232.0
MCP08B	sand-bed	MC3	<2 m	-1.75	-12.92	234.0
MCP10	sand-bed	MC3	<2 m	-4.13	-24.47	34.0
MCP03	sand-bed	MC1	<2 m	-0.11	-10.33	58.9
MCP03	sand-bed	MC1	<2 m	-3.58	-20.58	88.0
MCP03	sand-bed	MC1	<2 m	-3.47	-20.47	34.0
MCP04	sand-bed	-	<2 m	-3.54	-25.1	34.3
MCP04	sand-bed	-	<2 m	-1.88	-16.29	25.6
MCP04A	sand-bed	-	<2 m	-2.7	-19.79	56.5
MCP02	sand-bed	-	<2 m	-1.39	-13.56	18.3
MCP02E	sand-bed	-	<2 m	-3.79	-24.44	18.4
MC12D	bedrock	-	18-24 m	-5.04	-30.98	304.0
P3-16	bedrock	-	37-52 m	-4.73	-29.82	145.0
P3-3A	bedrock	-	40-52 m	-7.1	-44.92	111.0
P3-5	bedrock	-	29-41 m	-5.71	-35.38	252.0
P3-3B	bedrock	-	21-27 m	-5.19	-31.69	303.0
P3-3C	bedrock	-	10-16 m	-7.32	-46.47	98.0
P3-10B	bedrock	-	21-33 m	-5.53	-33.7	113.0
P3-15A	bedrock	-	42-54 m	-5.88	-36.62	234.0
P3-15B	bedrock	-	22-30 m	-7.3	-46.99	101.0
OB95-A	bedrock	-	57-61 m	-5.13	-31.51	416.0
OB95-B	bedrock	-	41-45 m	-5.06	-31.45	215.0
OB96-A	bedrock	-	35-38 m	-5.03	-31.16	159.0
MC27-D	bedrock	-	12-18 m	-3.82	-25.26	160.0

Table 2. Corrected xylem water isotope data. Species initials correspond to: LA: Lophopetalum arnhemicum; LG: Lophostemon grandiflora; LL: Lophostemon lactifluus; MA: Melaleuca alternifolia; MV: Melaleuca viridiflora.

Site	Landscape position	Species	$\delta^{18}O$ (‰)	δD (‰)
MC1	channel	LA	-2.27	-13.98
MC1	channel	LG	-2.88	-16.44
MC1	channel	LG	-1.46	-14.77
MC1	channel	MA	-1.43	-14.73
MC1	upper bank	MV	-3.29	-25.74
MC1	upper bank	MV	-1.25	-15.16
MC1	floodplain	MV	-2.53	-20.97
MC1	floodplain	MV	-2.48	-27.36
MC1	channel	LG	-3.00	-9.45
MC1	channel	LG	-2.45	-20.23
MC1	channel	MA	-3.00	-21.60
MC1	channel	MA	-2.49	-19.70
MC1	channel	MV	-2.20	-10.99
MC1	channel	MV	-1.98	-13.92
MC1	upper bank	LA	-2.20	-15.19
MC1	upper bank	LA	-2.59	-16.56
MC1	upper bank	LG	-2.15	-16.48
MC1	upper bank	LG	-2.73	-23.22
MC3	channel	LG	-0.91	-13.14
MC3	channel	LG	-1.13	-10.73
MC3	channel	LG	-3.20	-22.53
MC3	channel	LG	-1.41	-19.66
MC3	channel	MA	-2.74	-18.92
MC3	channel	MA	-3.02	-21.27
MC3	channel	MA	-2.35	-20.15
MC3	channel	MV	-3.30	-21.82
MC3	channel	MV	-2.46	-14.22
MC3	upper bank	LL	-1.68	-14.94
MC3	upper bank	LL	-1.51	-8.09
MC3	upper bank	LL	-1.50	-10.32
MC3	upper bank	LL	-1.72	-15.75
MC3	upper bank	MV	-1.66	-24.98
MC3	upper bank	MV	-2.04	-27.50
MC3	upper bank	MV	-2.71	-13.65

MC3	upper bank	MV	-3.30	-15.59
MC3	floodplain	LL	-2.76	-20.18
MC3	floodplain	LL	-1.84	-18.15
MC3	floodplain	LL	-1.45	-14.41
MC3	floodplain	MV	-4.73	-30.98
MC3	floodplain	MV	-5.01	-31.13
MC3	floodplain	MV	-4.70	-32.46

Table 3. Matric potential, gravimetric water content and corrected isotopic data obtained from soil profiles.

Site	Landscape position	Core #	Depth (m)	Matric potential (Mpa)	$\delta^{18}O$ (‰)	δD (‰)
MC1	upper bank	1	0.25	-12.76	6.56	2.16
MC1	upper bank	1	0.5	-12.46	-3.99	-28.66
MC1	upper bank	1	1.1	-0.76	-3.95	-25.55
MC1	upper bank	1	1.35	-0.67	nd	nd
MC1	upper bank	1	1.7	nd	-4.60	-31.25
MC1	upper bank	1	2.5	nd	-4.46	-32.39
MC1	upper bank	1	2.9	nd	-4.13	-26.19
MC1	upper bank	1	3.1	nd	-4.41	-27.62
MC3	channel	1	0.35	-18.99	-0.91	-19.04
MC3	channel	1	0.65	-2.18	nd	nd
MC3	channel	1	0.95	-1.29E-05	-2.75	-20.76
MC3	channel	1	1.15	-5.03E-06	-3.11	-22.31
MC3	channel	1	1.45	-1.44E-07	-2.63	-19.04
MC3	channel	1	1.7	-1.37E-09	-3.57	-22.29
MC3	channel	1	1.85	-1.01E-09	-2.91	-19.53
MC3	channel	2	0.25	-17.40	-0.30	-19.19
MC3	channel	2	0.75	-0.97	-0.90	-15.64
MC3	channel	2	1.15	-2.30E-04	-1.55	-15.66
MC3	channel	2	1.55	-3.06E-09	-3.96	-22.80
MC3	channel	2	1.85	-5.75E-10	-3.64	-22.84
MC3	channel	3	0.45	nd	-2.56	-17.24
MC3	channel	3	0.85	nd	-1.83	-21.95
MC3	channel	3	1.05	nd	-2.26	-20.14
MC3	channel	3	1.45	nd	-1.95	-16.89
MC3	channel	3	1.65	nd	-3.17	-19.90
MC3	channel	3	1.85	nd	-3.31	-20.07

MC3	upper bank	1	0.35	nd	0.58	13.05
MC3	upper bank	1	0.6	nd	-3.09	-16.44
MC3	upper bank	1	0.85	nd	-3.19	-15.91
MC3	upper bank	1	1.45	nd	-4.29	-27.92
MC3	upper bank	1	1.9	nd	-4.74	-28.20
MC3	upper bank	1	2.6	nd	-4.92	-30.26
MC3	upper bank	1	2.9	nd	-5.50	-34.02
MC3	upper bank	2	0.25	-18.59	-0.02	-14.14
MC3	upper bank	2	0.6	-3.42	-4.09	-20.40
MC3	upper bank	2	0.95	-5.59	-2.26	-16.69
MC3	upper bank	2	1.55	-8.21E-09	-3.71	-23.42
MC3	upper bank	2	1.95	-1.10E-07	-3.16	-18.45
MC3	upper bank	2	2.45	-6.31E-09	-4.67	-27.32
MC3	upper bank	2	2.63	-1.58E-09	-4.38	-26.46
MC3	upper bank	3	0.6	nd	-3.87	-28.30
MC3	upper bank	3	0.95	nd	-3.59	-24.09
MC3	upper bank	3	1.4	nd	-4.63	-27.86
MC3	upper bank	3	1.7	nd	-4.62	-26.13
MC3	upper bank	3	2.05	nd	-5.15	-30.90
MC3	upper bank	3	2.52	nd	-5.11	-30.38
MC3	floodplain	1	0.35	-7.69	-2.59	-17.88
MC3	floodplain	1	0.45	-6.03	-3.01	-18.49
MC3	floodplain	1	0.65	-1.09	nd	nd
MC3	floodplain	1	0.85	-1.23E-03	-4.21	-21.32
MC3	floodplain	1	1.1	-6.80E-06	-4.53	-28.98
MC3	floodplain	1	1.35	-9.13E-08	-4.83	-33.27
MC3	floodplain	1	1.65	-1.11E-08	-4.90	-38.34
MC3	floodplain	1	1.9	-1.10E-08	-4.84	-34.94
MC3	floodplain	1	2.35	-1.22E-08	-4.42	-33.52
MC3	floodplain	1	2.65	nd	-5.49	-32.60
MC3	floodplain	1	2.75	nd	-3.64	-25.06
MC3	floodplain	2	0.15	nd	2.01	-9.44
MC3	floodplain	2	0.3	nd	5.19	-1.77
MC3	floodplain	2	0.55	nd	-2.13	-22.78
MC3	floodplain	2	0.85	nd	-3.19	-28.35
MC3	floodplain	2	1.15	nd	-3.50	-21.85
MC3	floodplain	2	1.5	nd	-4.06	-27.61
MC3	floodplain	2	1.85	nd	-4.21	-27.05

MC3	floodplain	2	2.3	nd	-4.93	-28.47
MC3	floodplain	2	2.65	nd	-4.81	-28.46
MC3	floodplain	2	2.85	nd	-3.64	-24.97
MC3	floodplain	3	0.45	-7.42	-3.38	-17.14
MC3	floodplain	3	0.7	-0.03	-5.14	-29.33
MC3	floodplain	3	1.1	-1.12E-03	-4.99	-27.40
MC3	floodplain	3	1.5	-7.32E-07	-5.01	-26.84
MC3	floodplain	3	2	-1.41E-08	-5.22	-28.04
MC3	floodplain	3	2.3	-2.84E-09	-5.12	-28.46
MC3	floodplain	3	2.65	nd	-4.95	-28.62

Northern Australia Environmental Resources Hub

National Environmental Science Programme

CHARLES DARWIN UNIVERSITY AUSTRALIA

THE UNIVERSITY OF WESTERN AUSTRALIA

Australian Government

Department of Agriculture, Water and the Environment